



UNIVERSITY OF LEEDS

This is a repository copy of *MiR-19b non-canonical binding is directed by HuR and confers chemosensitivity through regulation of P-glycoprotein in breast cancer*.

White Rose Research Online URL for this paper:  
<http://eprints.whiterose.ac.uk/134974/>

Version: Accepted Version

---

**Article:**

Thorne, JL [orcid.org/0000-0002-3037-8528](https://orcid.org/0000-0002-3037-8528), Battaglia, S, Baxter, DE [orcid.org/0000-0001-8830-6802](https://orcid.org/0000-0001-8830-6802) et al. (8 more authors) (2018) MiR-19b non-canonical binding is directed by HuR and confers chemosensitivity through regulation of P-glycoprotein in breast cancer. *BBA - Gene Regulatory Mechanisms*, 1861 (11). pp. 996-1006. ISSN 1874-9399

<https://doi.org/10.1016/j.bbagr.2018.08.005>

---

© 2018 Elsevier B.V. All rights reserved. Licensed under the Creative Commons Attribution-Non Commercial No Derivatives 4.0 International License (<https://creativecommons.org/licenses/by-nc-nd/4.0/>).

**Reuse**

This article is distributed under the terms of the Creative Commons Attribution-NonCommercial-NoDerivs (CC BY-NC-ND) licence. This licence only allows you to download this work and share it with others as long as you credit the authors, but you can't change the article in any way or use it commercially. More information and the full terms of the licence here: <https://creativecommons.org/licenses/>

**Takedown**

If you consider content in White Rose Research Online to be in breach of UK law, please notify us by emailing [eprints@whiterose.ac.uk](mailto:eprints@whiterose.ac.uk) including the URL of the record and the reason for the withdrawal request.



[eprints@whiterose.ac.uk](mailto:eprints@whiterose.ac.uk)  
<https://eprints.whiterose.ac.uk/>

**MiR-19b non-canonical binding is directed by HuR and confers chemosensitivity through regulation of P-glycoprotein in breast cancer**

James L Thorne<sup>1\*</sup>, Sebastiano Battaglia<sup>2</sup>, Diana E Baxter<sup>3</sup>, Josie L Hayes<sup>4</sup>, Samantha A Hutchinson<sup>1</sup>, Samir Jana<sup>3,5</sup>, Rebecca A Millican-Slater<sup>6</sup>, Laura Smith<sup>3</sup>, Melina C Teske<sup>3</sup>, Laura M Wastall<sup>3,6</sup>, Thomas A Hughes<sup>3\*</sup>

<sup>1</sup>School of Food Science and Nutrition, University of Leeds, Leeds, UK

<sup>2</sup>Roswell Cancer Institute, Buffalo, USA

<sup>3</sup>School of Medicine, University of Leeds, Leeds, UK

<sup>4</sup>School of Public Health, University of California Berkeley, Berkeley, USA.

<sup>5</sup>Department of Zoology, University of Calcutta, Kolkata, India

<sup>6</sup>Department of Cellular Pathology, St James's University Hospital, Leeds, UK

\*Correspondence: tel +44 (0)113 3431984; email t.hughes@leeds.ac.uk; Wellcome Trust Brenner Building, St James's University Hospital, Leeds, LS9 7TF. Correspondence may also be addressed to j.l.thorne@leeds.ac.uk

## ABSTRACT

MicroRNAs and RNA-binding proteins exert regulation on >60% of coding genes, yet interplay between them is little studied. Canonical microRNA binding occurs by base-pairing of microRNA 3'-ends to complementary "seed regions" in mRNA 3'UTRs, resulting in translational repression. Similarly, regulatory RNA-binding proteins bind to mRNAs, modifying stability or translation. We investigated post-transcriptional regulation acting on the xenobiotic pump *ABCB1*/P-glycoprotein, which is implicated in cancer therapy resistance. We characterised the *ABCB1* UTRs in primary breast cancer cells and identified UTR sequences that responded to miR-19b despite lacking a canonical binding site. Sequences did, however, contain consensus sites for the RNA-binding protein HuR. We demonstrated that a tripartite complex of HuR, miR-19b and UTR directs repression of *ABCB1*/P-glycoprotein expression, with HuR essential for non-canonical miR-19b binding thereby controlling chemosensitivity of breast cancer cells. This exemplifies a new cooperative model between RNA-binding proteins and microRNAs to expand the repertoire of mRNAs that can be regulated. This study suggests a novel therapeutic target to impair P-glycoprotein mediated drug efflux, and also indicates that current microRNA binding predictions that rely on seed regions alone may be too conservative.

Keywords: breast cancer; post-transcriptional regulation; RNA-binding protein; miRNA; chemo-resistance; P-glycoprotein.

## 1 Introduction

Many different molecular mechanisms converge to regulate gene expression at post-transcriptional levels. Tight control of cellular protein levels is critical for regulation of protein function, and post-transcriptional control may allow particularly rapid responses to urgent stimuli (Patel et al., 2017) as well as providing overall fine-tuning of levels (Arcondeguy et al., 2013, Vallejo et al., 2011) and regulatory redundancy to reduce functional consequences of aberrant cellular signalling (He, 2010, Fischer et al., 2015).

MicroRNAs (miRNAs), a family of >1500 single-stranded RNAs of ~22 nucleotides in length, provide a prevalent mechanism of post-transcriptional control of protein expression (Griffiths-Jones et al., 2008, Griffiths-Jones, 2004), with the majority of mRNAs subject to their influence (Landgraf et al., 2007). The canonical pathway for miRNAs to exert regulation is via base-pairing to mRNAs within their 3' untranslated regions (UTRs). This binding typically comprises perfect base-pairing near the 5' end of the miRNA to a 6-8 nucleotide "seed region" in the target mRNA, with sparse pairing throughout the rest of the sequence (Wightman et al., 1993, Grimson et al., 2007). MiRNA binding results in loading of the mRNA into the miRNA Induced Silencing Complex (miRISC), leading to translational repression and/or mRNA destabilisation (Hammond et al., 2000). However, subtlety in these regulatory binding events is now evident, with some non-canonical miRNA-mRNA interactions being recognised (Flamand et al., 2017), meaning that classical seed region recognition does not cover the entire range of miRNA-induced regulation.

HuR (gene name *ELAVL1*) is a RNA-binding protein that increases the stability of its target mRNAs through binding to AU-rich elements within 3'UTRs (Mukherjee et al., 2011, Peng et al., 1998, Fan and Steitz, 1998). Interestingly, in addition to this well-characterised role through which HuR targets thousands of transcripts (Lebedeva et al., 2011), HuR has been shown to modify miRNA function for a few specific genes. A conceptually simple example of this is that HuR competes with miRNAs for binding to overlapping or adjacent mRNA target sites, resulting in inhibition of miRNA binding and up-regulation of expression (Lu et al., 2014). More complex, and poorly understood, is the observation that HuR can enhance binding of the miRNA let-7 to *MYC* transcripts, resulting in repression of c-myc translation (Kim et al., 2009). This cross-talk between RNA-binding proteins and miRNAs underlines the potential complexity of interactions between different regulatory molecules that converge on the 3'UTR.

P-glycoprotein (P-gp; gene name *ABCB1*) represents a notable paradigm as a target of extensive post-transcriptional regulation. Post-transcriptional regulatory mechanisms that act on it include usage of alternative 5'UTRs with differing secondary structures and consequences for expression (Randle et al., 2007), alternative 3'UTRs and polyA sites (Hsu et al., 1990), and binding by stability modulating RNA-binding proteins (Boyerinas et al., 2012) or miRNAs (Bao et al., 2012, Kovalchuk et al., 2008). Importantly, P-gp is critically involved in the response of many cancer types to chemotherapy (Ueda et al., 1987), especially the response of breast cancer (Turton et al., 2001, Trock et al., 1997, Tulsyan et al., 2016). P-gp is capable of exporting a range of xenobiotics from cells and is found over-expressed in drug-resistant breast cancer cell lines and in primary breast tumours, especially when exposed to chemotherapy (Kim et al., 2013). However, therapeutics designed to enhance

chemotherapy responses based on inhibition of P-gp protein function have broadly failed (Crowley et al., 2010), due in part to side-effects linked to P-gp's critical role in normal physiology. Therefore, furthering understanding of post-transcriptional regulation of P-gp in cancer is of considerable interest both as a paradigm of regulatory complexity, and in order to identify cancer-specific regulation that could allow therapeutic manipulation of P-gp expression. Our aim here was to identify sequences and mechanisms allowing post-transcriptional regulation of P-gp expression in breast cancers with a view to satisfying both these areas of interest.

## **2. Materials and Methods**

### ***2.1 Rapid amplification of cDNA ends (RACE)***

Ethical approval was obtained from Leeds East research ethics committee (09/H1306/108). RNA was extracted using Reliaprep (Promega; Madison, WI, USA) from four primary breast samples comprising non-tumour, and tumours of subtypes luminal A, luminal B, and triple negative basal-like. 5' and 3' RACE was performed using kits from Invitrogen (Carlsbad, CA, USA) following the manufacturer's protocols and using primers listed in Table S1. Products were analysed by agarose gel electrophoresis (Tris-acetate EDTA buffer), excised under UV visualization, extracted using Zymed DNA gel extraction kits, and cloned into TA cloning vectors (both Invitrogen; Carlsbad, CA, USA). Inserts were sequenced using the BigDye™ Terminator Sequencing Kit (Thermo Fisher; Waltham, MA, USA).

### ***2.2 Cloning and site directed mutagenesis***

To generate the ABCB1 "full 5'+3'" GFP reporter construct, the ABCB1 5'UTR was first cloned into pTH-GFP immediately upstream of the GFP ORF and downstream of the CMV promoter. The bulk of the 5'UTR encoded by exon 1b (see Fig 2) was amplified by PCR from genomic DNA using a forward primer with an added SacI site and a reverse primer with an added Sall site. The PCR products were cloned into pTH-GFP using SacI/Sall (New England Biolabs; MA, USA) to generate 5'-UTR-pTH-GFP. The ABCB1 3'UTR sequences were amplified by PCR from genomic DNA with BamH1 added to a common forward primer and HindIII added to each of the reverse primers in order to generate full 5'+3' and  $\Delta 1$ . Fragments were cloned BamH1/HindIII into 5'-UTR-pTH-GFP to generate constructs with the GFP ORF flanked by ABCB1 UTRs. Correct sequence insertion was confirmed in both directions by sequencing as above.

The region of the 5'UTR encoded by exon 2 (see Fig 2) was then added using the Q5 Site Directed Mutagenesis kit (E0554S New England Biolabs; MA, USA) with primers designed using the manufacturer's online design tool. Mutation of the canonical miR-19b site was performed using Q5 SDM, changing the seed region from TTTGCATA to ATAGCTAA. Deletion constructs  $\Delta$ 2-6 were generated with a common forward primer and a series of reverse primers at 50bp intervals culminating in complete deletion of the ABCB1 3'UTR for the  $\Delta$ 6 construct. All primer sequences are detailed in Table S1.

### ***2.3 Cell culture and transfections***

Cell lines were obtained originally from the European Collection of Animal Cell Cultures. Cell line identities were confirmed (STR profiles, Leeds Genomics Service) and lines were consistently negative for mycoplasma (MycoAlert Mycoplasma detection assay, Lonza, Basal, Switzerland). MCF7 and HB2 cells were maintained in DMEM supplemented with 10% FCS (Thermo Fisher; Waltham, MA, USA) and maintained between 20 and 80% confluence. Transfections for translational efficiency were performed in duplicate wells of a 6-well plate using Lipofectamine 2000 (Thermo Fisher; Waltham, MA, USA) according to manufacturer's guidelines. 900ng of pcDNA3.1 empty vector was used as a carrier for 100ng of GFP reporter (amount of each reporter was corrected for its size in base pairs relative to the GFP control to ensure equi-molar transfections) mixed in Optimem (Thermo Fisher; Waltham, MA, USA) with Lipofectamine 2000 at 7.5:1 ratio. MiR-inhibitors, mimics and controls were purchased from Thermo Fisher (Waltham, MA, USA) and were used at final concentration of 30nM (miR-19b inhibitor: 4464084; inhibitor control: 4464076; miR-19b mimic: 4464066; mimic control: 4464058). SiRNA were purchased from Santa-Cruz (Dallas, TX, USA) and were used at final concentration of 10nM (siHuR: sc-35619; siControl: sc-37007). Assays were performed in duplicate wells of a 6-well

plate on  $2.5 \times 10^5$  cells using 5 $\mu$ l RNAiMAX following manufacturer's protocols (Thermo Fisher; Waltham, MA, USA). For co-transfection, 900ng pcDNA3.1 carrier and 100ng GFP reporter were combined with miR-inhibitor or control, or siRNA, and mixed with RNAiMAX in Optimem. For HB2 cells, transfection complexes were added to cells in the absence of serum. All transfection complexes were incubated with cells for 16h before replacing with fresh medium, and were performed on  $2.5 \times 10^5$  cells/well of a 6-well plate, except for siHuR pull-down experiments where a 50% confluent T150 tissue culture flask was used.

#### ***2.4 Expression analysis of mRNA and miRNA in cell lines***

For mRNA expression analysis, RNA was isolated using RNeasyprep kits and reverse transcribed using GoScript (both from Promega; Madison, WI, USA) with oligo-dT primers. qPCR was performed in duplicates with 300nM primers (sequences: Table S1) and GoTaq SYBR Green PCR Master Mix (Promega; Madison, WI, USA) on the 7500HT qPCR machine (Applied Biosystems; Warrington, UK). Expression was normalised to reference gene 36B4 using the  $\Delta\Delta$ Ct method (Satheesha et al., 2011). For miRNA expression analysis, RNA was extracted using the mirVana miRNA Isolation Kit (Thermo Fisher; Waltham, MA, USA) and miRNAs were reverse-transcribed with gene specific primers (Thermo Fisher; Waltham, MA, USA). qPCR analyses were performed on 7500HT machines (Applied Biosystems; Warrington, UK) in triplicate using gene specific Taqman assays (Thermo Fisher; Waltham, MA, USA). Relative miRNA expression was determined using  $\Delta\Delta$ Ct against the geomean of normalisers U6 and RNU48.

#### ***2.5 Translational efficiency assay***

We have described this assay in detail previously (Smith et al., 2010b, Satheesha et al., 2011). In brief, relative GFP protein and mRNA levels were used to assess GFP protein produced per unit mRNA. Illustrative data for GFP protein expression, and GFP mRNA levels are shown in Fig S1. Following transfection, RNA was purified using RNeasy (Qiagen; Crawley, UK) with on column DNase digestion followed by two additional TURBO DNase I digestions (Thermo Fisher; Waltham, MA, USA). cDNA was synthesized and analysed as above. For analysis of GFP protein expression, cells were suspended in phenol-red free RPMI with 1% FCS and fluorescence quantified (geometric mean fluorescent intensity of  $2.5 \times 10^5$  events after exclusion of debris/dead cells on forward activated light scatter/side scatter) at 525 nm using an LSR II machine (BD Biosciences; Oxford, UK).

## **2.6 Western blots**

Proteins were extracted using RIPA buffer (10mM Tris-HCl pH8, 140mM NaCl, 0.1% SDS, 1% Triton X-100, 0.1% sodium deoxycholate, 1mM EDTA, 0.5mM EGTA) with 1mM PMSF and 1mM DTT added immediately prior to use. Without prior heating proteins were loaded onto Novex 4-12% gradient gels (Thermo Fisher; Waltham, MA, USA), transferred to PVDF membranes, and blocked (P-gp: 5% milk 30min followed by 1% milk 45min; actin: 5% milk). Proteins were probed with anti-Pgp C219 (EMD Millipore; Billerica, MA, USA; 1/100 overnight at 4°C), anti-HuR D9W7E rabbit monoclonal (cat. number 12582, Cell Signalling Technologies; Danvers, MA, USA; 1/500 overnight at 4°C), or mouse anti- $\beta$ -actin (A5441, Sigma; Gillingham, Dorset - or - 8H10D10, cat. number 3700, Cell Signalling Technologies; Danvers, MA, USA; both at 1/10,000 overnight at 4°C). They were then blocked and probed in 1% milk with HRP-conjugated secondary antibodies (Santa Cruz Biotech; CA, USA) at 1/10,000, and signal was visualised with West Pico (Thermo Fisher; Waltham, MA, USA), or with

secondary antibodies (IRDye 800CW goat anti-mouse cat. number 926-68170, IRDye 680RD donkey anti-rabbit cat. number 926-68171; LI-COR; Lincoln, NE, USA) and image acquired using LI-COR equipment (LI-COR; Lincoln, NE, USA).

### **2.7 MiRNA in silico screening**

208 miRNAs were predicted to bind to the longest *ABCB1* 3'UTR (NM\_000927) according to microRNA.org, and these were included in the initial analysis. miRNAs with duplex free energies of  $>-9$  were excluded so as to account for poor site accessibility (Kertesz et al., 2007), a single wobble and a single mismatch were allowed, and a minimum seed region of 6 was specified. MiRNAs under further consideration were limited to those expressed in breast tumour tissue, and those demonstrating a significant inverse correlation (greater than coefficient 0.2) with *ABCB1* mRNA in breast tumour tissue (TCGA data (Cancer Genome Atlas, 2012) downloaded via the cBioPortal platform (Cerami et al., 2012, Gao et al., 2013).

### **2.8 Molecular pathology: immunohistochemistry and laser micro-dissection/qPCR**

Ethical approval was obtained from Leeds East research ethics committee (06/Q1206/180, project specific; 09/H1306/108, Leeds Breast Tissue Bank). 9 cases of invasive ductal breast carcinoma of no special type, where matched normal-adjacent, DCIS and invasive carcinoma appeared within the same archival (formalin-fixed, paraffin-embedded) block, were identified and marked up by consultant breast histopathologist RM-S from haemotoxylin and eosin stained slides. The histopathological details for these individuals/tumours have been described in Table 1 of a previous publication (Smith et al., 2015). All patients were chemotherapy naïve at the time of resection. For analysis of protein expression, immunohistochemistry was

performed as previously described (Kim et al., 2013). Briefly, tissues were sectioned at 5µm onto SuperFrost Plus slides (Menzel-Glaser; Braunschweig, Germany). Sections were dewaxed and rehydrated. Epitope retrieval was not performed. Endogenous peroxidase activity was blocked using 0.3% H<sub>2</sub>O<sub>2</sub>. Non-specific binding activity was blocked using casein solution (SP5020 Vector Labs; Burlingame, USA). Slides were incubated with anti-Pgp (sc-73354 Santa Cruz Biotech; CA, USA) at 1:2000 in antibody diluent solution (Invitrogen, Paisley, UK) for 1h at room temperature. Staining was visualised using Envision reagents (Dako; Gostrup, Denmark). Sections were stained in Mayer's haematoxylin, dehydrated and mounted in DPX (Fluka; Gillingham, UK). Sections were digitally scanned using Scanscope XT and were observed and analysed using Imagescope (Aperio; Vista, CA, USA). The mouse monoclonal antibody against P-gp used here has been used previously for IHC on breast tissue by us and others (Mechetner et al., 1998, Kim et al., 2013) and its specificity has been validated previously using Western blotting on breast cell lines - (Mechetner and Roninson, 1992). Positive staining within breast epithelial cells (normal, DCIS, or invasive cancer) was assessed semi-quantitatively. Weighted histoscores (van Nes et al., 2012) were generated by two independent observers (JLT, and LMW [a histopathologist]). The observers counted and quantitatively assessed staining in the same 3 separate high power fields. Histoscores (of 0–300) were (1×% of tumour cells weakly stained)+(2×% moderately stained)+(3×% strongly stained). The inter-observer intraclass correlation coefficient (ICC) for the independent scoring was 0.86 (Fig S2), which represents 'almost perfect agreement' (Barry et al., 2010). The average score for each sample from the two observers was used for analyses. For analysis of miRNA expression, laser micro-dissection of epithelial breast cells was performed as previously described (Verghese et al., 2013) using a Zeiss/PALM microdissection microscope and 10µm sections. Areas of 5-10mm<sup>2</sup> for

each compartment of normal, DCIS or invasive cells (as identified above) were digitally outlined and cells were collected in sterile adhesive caps. Areas selected were devoid of visible cells other than epithelial cells. Representative images of this microdissection have been published as Figure 2 in a previous publication (Smith et al., 2015). RNA was extracted using the mirVana miRNA Isolation Kit (Thermo Fisher; Waltham, MA, USA) and miRNAs were reverse-transcribed and pre-amplified using the MegaPlex RT primers and pre-amplification (Thermo Fisher; Waltham, MA, USA). qPCR analyses were performed on 7500/7900HT machines (Applied Biosystems; Warrington, UK) in triplicate with Taqman assays (Thermo Fisher; Waltham, MA, USA). Relative miRNA expression was determined using the geomean of normalisers U6 and RNU48.

### ***2.9 RNA immuno-precipitation assay***

$2 \times 10^7$  MCF7 cells per immuno-precipitation were washed in ice cold PBS twice before resuspension in a volume equal to the size of the pellet of ice-cold CLB (100mM KCl, 5mM MgCl<sub>2</sub>, 10mM HEPES pH7, 0.5% NP40) supplemented with 1mM DTT and 100U/ml of RNase Out (Promega; Madison, WI, USA), Protease Inhibitor Cocktail (1697498 Roche; Basel, Switzerland) and protein phosphatase inhibitor at time of use. Cells were mixed and left on ice for 10 min. Lysates were spun and supernatant collected in a fresh tube for pre-clear with IgG1 bound to Dynabeads Protein G (Thermo Fisher; Waltham, MA, USA) following the manufacturers recommendations. Lysates were diluted in 800µl PLB buffer with additives and 30µl of HuR ([D9W7E] New England Biolabs; MA, USA) or IgG ([DA1E] New England Biolabs; MA, USA) bound beads in 100µL NT buffer (50mM TRIS pH 7.4, 150mM NaCl, 1mM MgCl<sub>2</sub>, 0.05% NP40 with RNase inhibitor). The mixture was rotated end over end for 4h at 4°C followed by 5 washes in 1ml aliquots of NT2 buffer. Beads were then

resuspended in 100µl NT2 with 10U DNase I at 37°C for 10 min. Supernatant was discarded and for mRNA extraction beads resuspended in BLTG (Promega; Madison, WI, USA), or for miRNA extraction in miRVana buffer (Thermo Fisher; Waltham, MA, USA).

### **2.10 UTR pull-down assay**

50µl of MyONE C1 Dynabeads (Thermo Fisher; Waltham, MA, USA) were mixed with 250pmol of oligos (Sequences: Table S1) biotinylated at the 5' end corresponding to either the responsive (R; positions 5-54) or non-responsive (nR; positions 55-104) regions (Integrated DNA Technologies; Leuven, Belgium) for 12 min at 37°C with gentle rotation. Beads were then washed in WB (5mM Tris-HCl pH 7.5, 0.5mM EDTA, 1M NaCl, 0.05% Tween) and resuspended in 50µl NT buffer. Lysates were extracted from MCF7 cells by resuspending in PLB as above, in the presence or absence of Queretin at 10µM, or after transfection with siHuR or siControl. 850µl of NT buffer was added to 100µl cell lysate in PLB, and 50µl set aside for input sample. 50µl of bead-oligo complex was added and the mixture incubated for 2 h at room temperature with end-over-end rotation. Beads were washed three times in NT buffer, and resuspended in 20µl TE (1mM EDTA pH 7.5, 10mM Tris-HCl pH 7.5). This was heated to 70°C at 0.5°C/s, and then immediately allowed to return to room temperature. Supernatant containing the eluted RNA was resuspended in miRVana buffer.

## **3 Results**

### **3.1 ABCB1 UTRs are single majority species with little variation across different breast epithelial cells**

In order to investigate post-transcriptional regulation of *ABCB1*/P-gp in breast cancer, our aim was first to identify accurately the UTR sequences expressed on *ABCB1* transcripts in breast epithelial cells, as the UTRs act as targets for most post-transcriptional regulation. “Rapid amplification of cDNA ends” (RACE) was employed to amplify *ABCB1* UTRs from samples of normal breast tissue, a luminal A primary breast cancer, a basal primary breast cancer, and the MCF7 breast cancer cell line, and these were then cloned and sequenced.

At the 3' end of the transcript, three different species were identified as common to each sample (Fig 1A). Sequencing revealed that these represented different lengths of 3'UTR, aligning with the 3' of exon 29 (the final coding exon of the gene), and each terminating at different alternative polyadenylation sites (Fig 1B). Product 1 was produced from the most 3' polyadenylation site therefore generating the longest UTRs (a range of 378-384 bases for individual molecules), product 2 was shorter (a broader range of 242-298 bases), and product 3 represented the most proximal polyadenylation event (119 bases). Notably, we did not identify expression of an even longer potential 3'UTR previously investigated by Bao et al and Kovalchuk et al, potentially produced by polyadenylation further downstream (p(A)long; Fig 1B) (Bao et al., 2012, Kovalchuk et al., 2008). The lack of this species is of relevance as expression from it is apparently regulated by miR-298 (Bao et al., 2012) or miR-451 (Kovalchuk et al., 2008) in breast cancer. When interpreting these data, it was important to consider that RACE does not give relative quantitation of species because of variation in product amplification dynamics. Therefore, we next used qPCR to assess relative expression of UTRs compared to the *ABCB1* open reading frame (Fig 1C). In all samples, the UTR produced from polyadenylation site 1 (labelled “1”) accounted for the vast majority of transcripts. We were unable to detect any

expression above background of the potential longer UTR (“long”) (Bao et al., 2012, Kovalchuk et al., 2008), with background defined as expression from 5kb downstream of the gene (“d/s”). Unfortunately, we were not able to design specific primers to assess expression of the shorter UTRs because of the repetitive and AU-rich nature of the sequence. Nevertheless, we concluded that the majority of *ABCB1* 3’UTRs in breast epithelial cells are between 378-384 bases long, as encoded by exon 29.

We also performed similar analysis of 5’UTRs (Fig 2). We observed only a single RACE product (Fig 2A), the start of which aligned close to the previously reported exon 1b (Fig 2B), although the transcriptional start site (TSS 1) was apparently 12-14 bases further 3’ than previously reported (Ueda et al., 1987) (full sequence in Fig S3). An upstream transcriptional start site (TSS -1) has previously been reported in breast cells, allowing expression of sequences from exons -1 and 1a (grey in Fig 2B) (Chen et al., 1990), however we did not identify their expression by RACE. qPCR was again used to give quantitative insights (Fig 2C), and this confirmed that expression of exon 1b accounted for the vast majority, or even an excess, of transcripts relative to the open reading frame, while expression of sequences from TSS -1 (labelled “-1” and “1a”) was negligible. We concluded that 5’UTRs in breast cells are overwhelmingly 129-131 bases in total, encoded by exon 1b spliced to the first coding exon (exon 2).

### ***3.2 MiR-19b expression inversely correlates with ABCB1 and P-gp expression in breast cancer***

Next, we were interested to identify miRNAs that could potentially act on these UTRs. Initially, we performed an *in silico* screen using bioinformatics predictions of miRNA binding and using publically available gene expression datasets. MiRNAs that were predicted to bind to the majority *ABCB1* 3’UTR identified above were identified using

tools at microRNA.org, with defined criteria for strength and nature of the predicted interaction (see methods); 81 different miRNAs were identified that were predicted to bind at 146 different seed regions. MiRNAs of interest were further reduced to 49 by focusing only on those expressed in breast tumours, as assessed from TCGA breast tumour expression dataset (ATLAS, 2012). Finally, since miRNAs can cause reduced stability in their target mRNAs, we tested for negative correlations between expression of miRNA and ABCB1 transcript. We identified 8 that showed a significant correlation of at least -0.2 (weak) in Pearson rank correlation tests. These were let-7a and miR-19a, -19b, -30c, -34a, -148b, -200c, and -455; predicted binding characteristics and correlations with *ABCB1* are shown in Table S2 and Fig S4 respectively.

This *in silico* screen had two notable drawbacks. Firstly, the expression data used are from whole tissue samples, containing variable and likely considerable contributions from stromal cells as contaminants for assessment of epithelial expression. Secondly, analysis was limited to transcripts, which does not take into consideration miRNA translational inhibition capability, as protein expression would. In order to address these concerns, we carried out further screening. We identified 9 breast cancer cases (histological subtype: ductal carcinoma, no special type) where matched invasive carcinoma, pre-invasive ductal carcinoma in situ (DCIS), and normal epithelial cells were present. Epithelial cells of each of these three types were purified by laser microdissection from tissue sections, allowing assessment of expression of our 8 miRNAs of interest in these epithelial compartments by qPCR (Fig 3A). In addition, P-gp protein expression was detected in matched tissue sections using immunohistochemistry and was quantified as histoscores in the same epithelial compartments (Fig 3B). Of note was that miR-19b expression was significantly lower in invasive cancer cells when compared to matched normal cells ( $p < 0.05$ ) hinting at a

potential tumour suppressor role for miR-19b, with no other miRNAs showing significant differences. In addition, P-gp expression was progressively up-regulated during cancer development from normal cells, through matched DCIS ( $p < 0.01$ ), to matched invasive cancer ( $p = 0.01$ ). Finally, correlations between miRNAs and P-gp protein were tested (Fig 3C); miR-19b and P-gp showed the only significant correlation, with a correlation coefficient of  $-0.36$  ( $p < 0.05$ ). We concluded that miR-19b is a strong candidate as a negative regulator of ABCB1/P-gp in breast cancer.

### **3.3 MiR-19b regulates P-gp expression and influences chemotherapy response**

Next, we performed functional experiments in breast cell lines to investigate whether miR-19b has direct regulatory influences on ABCB1/P-gp expression and function. MiR-19b mimics or control non-targeting mimics were transfected into MCF7 cells (a representative luminal A breast cancer cell line) or HB2 cells (immortalised breast epithelial cells from a non-cancer origin) and Western blots were performed to quantify P-gp and qPCR to quantify ABCB1 transcript (Fig 4A). P-gp protein expression was strongly reduced by miR-19b over-expression, while ABCB1 transcript levels were not significantly altered (although there was a suggestion of up-regulation in HB2 cells); this change at the level of protein but not mRNA was potentially indicative of regulation at the level of translation. Furthermore, MCF7 cells transfected with miR-19b mimic showed significantly increased drug loading when treated with the chemotherapeutic doxorubicin as assessed using flow-cytometry ( $p < 0.004$ ), and reduced survival after treatment with doxorubicin in colony forming assays ( $p = 0.028$ ; Fig 4B), results indicative of reduced P-gp function. We concluded that miR-19b regulates P-gp expression and function.

A reporter assay was employed to establish whether *ABCB1*/P-gp was a *direct* target of miR-19b, acting at the level of translational regulation (Smith et al., 2010a, Smith et al., 2010b, Satheesha et al., 2011). A reporter was constructed to allow over-expression of transcripts with both the 5' and 3'UTRs identified above as the prevalent species in breast cells flanking the GFP open reading frame; this reporter is termed "full 5'+3'". This was compared to a control reporter ("con") lacking these specialised UTR sequences. MCF7 or HB2 cells were transfected with these reporters along with miR-19b inhibitor or an inhibitor control, and translational efficiency of GFP messages was assessed, by measuring the ratio of GFP fluorescence to GFP mRNA (Fig 4C). Note that this assay is insensitive to regulation acting at the level of mRNA stability, as protein is assessed relative to amounts of mRNA, and to changes in target protein stability, as a reporter protein is used. Under control conditions, the full 5'+3' reporter demonstrated significant inhibition of translational efficiency by 50-70% as compared to the non-specialised UTR reporter ( $p < 0.01$ ; compare open bars in each panel). Inhibition of miR-19b caused significant and almost complete derepression of translation ( $p < 0.02$ ; compare full 5'+3' open and filled bars), demonstrating that miR-19b directly targets the *ABCB1* UTRs, and that its expression is required for these UTRs to specify strong translation repression. Therefore, we concluded that miR-19b regulates P-gp/*ABCB1* expression at the levels of translation (Fig 4C), and – potentially in cancers - mRNA stability (Fig S4). As an interesting aside, the 5'UTR contains two SNPs, rs2214102 and rs3213619, at positions -1 and -127 relative to start codon. Both variants are represented in the population at frequencies of approximately 10% (Poupon et al., 2008, Calado et al., 2002). The minor allele at rs2214102 associates with reduced survival in breast cancer patients (Vaclavikova et al., 2012) and the minor allele at rs3213619 associate with decreased P-gp expression (Tanabe et al., 2001) and decreased chemotherapy clearance (Yamaguchi

et al., 2006). However, the variants (alone or in combination) did not impact directly on translational efficiency, even though rs2214102 is within the Kozak translational start consensus (Fig S5).

### ***3.4 The canonical miR-19b seed region is dispensable for miR-19b dependent translational repression***

We next wanted to assess whether the canonical miR-19b binding site, seed region bases 340 to 347 within the most prevalent 3'UTR, was directly responsible for miR-19b mediated translational repression as might be expected. To this end, the miR-19b seed region was mutated within the full 5'+3' reporter, to destroy the canonical miR-19b site (5'-TTTGCATA-3' changed to ATAGCTA [Fig 5A]). Contrary to our expectations, translational repression was not alleviated by the mutations, and inhibition of miR-19b continued to derepress translation (Fig 5B). To analyse this unexpected observation further, the binding site was entirely removed, by deletion of the most 3' 50 bases from the 3'UTR of the reporter ( $\Delta 1$  construct; see Fig 5C). As before, this did not result in derepression of translation under control conditions, or in loss of sensitivity to miR-19b inhibition (Fig 5D). We concluded that the canonical miR-19b site was not responsible for the miR-19b dependent regulation. A series of progressively larger 3' deletions were made within the reporter in order to identify the UTR region responsible for the miR-19b mediated translational repression (Fig 5C). Derepression was not seen with constructs  $\Delta 2$  through to  $\Delta 5$  (Figs 5E-F) and the smallest of these constructs,  $\Delta 5$ , with only 54 bases of 3'UTR remaining, remained responsive to inhibition of miR-19b ( $p < 0.001$ ). However, a final deletion of the entire *ABCB1* 3'UTR did result in a significant derepression ( $p = 0.002$ ), and loss of response to miR-19b inhibition. We concluded that the 54 bases of 3'UTR in the  $\Delta 5$  construct must contain elements capable of responding to miR-19b.

### ***3.5 HuR is required to load miR-19b onto the 3'UTR at a non-canonical site and to direct translational repression***

We examined potential binding sites within this 54 base sequence manually, testing for poor sites that would not meet automated consensus searches. We noted it contained an extremely poor potential binding site for miR-19b, with 14 complementary bases, 7 mismatches, 2 G/T wobbles and one bulge over the entire miRNA 21 base sequence, but no recognisable seed region. The predicted binding free energy was calculated with UNAFold (Markham and Zuker, 2008) (see Fig S6 for the predicted binding structure) as only -7.9kcal/mol, which is considerably less favourable than a typical canonical predicted miR-19b site (eg -13.7kcal/mol for the site further down-stream in this UTR). The binding was so poor that we have not been able to identify it with any prediction tools (miRWalk, microRNA.org, miRanda, Pictar2, Targetscan). We also noted that this potential binding site overlapped with a strong consensus binding site (Lopez de Silanes et al., 2004) for the RNA-binding protein HuR (Fig 6A).

First, we investigated whether this 3'UTR sequence could potentially bind miR-19b. We performed a pull down experiment using biotinylated RNA containing the potential binding site (3'UTR bases 3-52, the miR-19b responsive section; "R") and compared this, as a control, to an adjacent section of the same 3'UTR of a similar length (bases 67-116, non-responsive; "non-R") for which there was no suggestion of translational repression activity (see Fig 5). We used qPCR to assess whether these sequences were able to bind endogenous miR-19b from lysates of MCF7 cells. MiR-19b was significantly recovered on the responsive RNA sequence ( $p < 0.001$ ; Fig 6B). We also assessed whether HuR expression or activity was required for this miR-19b binding.

Specific binding of miR-19b to the responsive sequence was completely abolished when endogenous HuR expression was reduced by transfection with siRNA, or when cellular HuR activity was inhibited with the flavonoid quercetin that reduces HuR binding to its AU-rich target sites (Chae et al., 2009) (Fig 6B). We also confirmed the efficacy of the siRNA knockdown of HuR by qPCR and Western blot (Fig 6C).

Next, we assessed whether HuR could bind, either directly or indirectly, to miR-19b, again using endogenous molecules where possible. An experimentally validated antibody against HuR (Zhu et al., 2016, Chu et al., 2013) was chosen to immunoprecipitate HuR complexes from MCF7 lysates, and recovery of miR-19b was assessed, relative to a control immunoprecipitation (Fig 6D). Endogenous miR-19b was pulled down by immunoprecipitation of endogenous HuR as compared to control. Finally, we examined whether HuR expression impacted on the translational repression associated with the *ABCB1* UTRs. MCF7 cells were co-transfected with the reporter construct allowing expression of the minimal miR-19b responsive translational repression sequences, the  $\Delta 5$  construct, along with either HuR targeted siRNA or control non-targeting siRNA (Fig 6E). Reduced HuR expression (see Fig 6C) was associated with translational derepression (Fig 6E), similarly to inhibition of miR-19b itself (see Fig 5D). Overall, we concluded that HuR was required to allow miR-19b to bind to this non-canonical binding site, and thereby repress translation of P-gp. As a final test, we examined whether HuR (*ELAVL1*) expression correlated with *ABCB1* expression in publically available gene expression datasets for breast cancer. HuR (*ELAVL1*) showed a significant negative correlation with *ABCB1* expression (Spearman's rho -0.32,  $p < 0.0001$ ; Fig S7), in accordance with the role we have defined in loading miR-19b onto *ABCB1* and thereby destabilising the transcript, and

in marked contrast to the well-understood role of HuR as a RNA-stabilising factor (for which a positive correlation would be expected).

#### **4. Discussion**

We set out to investigate post-transcriptional regulation of the multi-drug resistance gene *ABCB1/P-gp* in breast cancer. We have used a number of thorough approaches, which we believe had a critical influence on our findings, and explain why these differ from some published data. An example of this is our use of RACE and qPCR reactions to identify and quantify the UTRs expressed in our cells of interest (Fig 1 and 2). This step appears to be surprisingly rare in studies of post-transcriptional regulation, despite widespread differential expression of alternative 5'UTRs (Hughes, 2006), through multiple transcriptional start sites or alternative splicing, and 3'UTRs (Di Giammartino et al., 2011) through use of alternative polyadenylation sites. Of note is the fact that using this approach we have failed to identify as significantly expressed regulatory sequences previously reported as of interest in breast cancer (Bao et al., 2012, Raguz et al., 2008, Kovalchuk et al., 2008), thereby casting doubt on their physiological relevance. A second example is our screening strategy to identify potential miRNA regulators of P-gp. We have started, as is typical, with bioinformatics predictions of binding to the 3'UTR, but we have supported this with an analysis of potential negative correlations between miRNA and target at mRNA level and protein level in two separate groups of patient samples, as well as subsequent functional work in cell lines mapping the relevant binding sites. We hope that this strategy increases our chances of identifying regulation that both can occur in both experimental systems, and *in vivo*. Finally, we have used laser microdissection to isolate epithelial cells from tissue samples, thereby limiting our analysis to the specific cells of interest. This may explain why we found miR-19b to be significantly down-regulated during

cancer progression (Fig 3A), while it has previously been found to be up-regulated in breast cancer as compared to matched normal samples using whole tissues (Li et al., 2017).

Through these analyses, we have identified miR-19b and HuR as novel negative regulators of *ABCB1*/P-gp in breast cancer, acting at the levels of translational regulation (Fig 4) and, potentially, mRNA stability (Fig S4). Of note is the fact that the negative correlations between *ABCB1* and these two regulators are also present in prostate cancer, but not in colorectal or lung cancers, hinting at regulation that may be specific to certain tumour types (Fig S8). Regulation of *ABCB1* by HuR is further supported by the fact that it has previously been identified as a direct HuR target using pull-down and sequencing approaches (Mukherjee et al., 2011). MiR-19b has been implicated as a potential oncomiR in many cancers (Olive et al., 2009, Jin et al., 2013), and it has been assigned potential cancer-promoting functions in breast cancer via negative regulation of tumour suppressor genes such as *PTEN* (Li et al., 2014), *PTPRG* (Liu et al., 2016) and *BRCA2* (Mogilyansky et al., 2016). In contrast, our data support a tumour suppressor role for miR-19b in breast epithelial cells, in accordance with some data in prostate cancer (Ottman et al., 2016) and hepatocellular carcinoma (Hung et al., 2015). HuR has also been defined as an oncogene, with higher expression associated with poor survival in breast and other cancers (Zhu et al., 2013, Denkert et al., 2004, Wang et al., 2013), and it is the focus of ongoing work to develop novel targeted therapeutics (Huang et al., 2016, Muralidharan et al., 2017, Wu et al., 2015). Strangely, expression levels of HuR and P-gp have previously been shown to correlate positively in breast cancer (Zhu et al., 2013), in direct contrast to the regulation we have identified, although this previous observation may be compromised by the lack of antibody validation.

Most interestingly, we established that miR-19b regulates *ABCB1*/P-gp via non-canonical miRNA binding in concert with adjacent binding of HuR. In this role, HuR binding does not lead to mRNA stabilisation as is typical (Mukherjee et al., 2011), but facilitates loading of miR-19b to the adjacent non-canonical site thereby allowing miR-19b-dependent down-regulation of P-gp expression. Of note is the fact that the paired miR-19b/HuR sites appear to be conserved in both murine homologs of the *ABCB1* gene, *Abcb1a* and *Abcb1b* (Fig S9). Within the literature, we have identified one related observation, in which HuR similarly stabilised the loading of the miRNA let-7 to the *MYC* 3'UTR (Kim et al., 2009), although in this example the miRNA binds to a canonical site and its binding is stabilised, rather than HuR allowing use of a site that is otherwise not suitable, as we see with *ABCB1*. From our data, we are not able to comment on whether HuR directly binds to these miRNAs in the absence of the target mRNAs, however HuR has been reported to bind directly to miR-21, in this case apparently acting as a microRNA 'sponge' (Poria et al., 2016). While HuR-induced loading of miRNAs remains exceptional within the literature, we believe HuR-induced loading of miR-19b may be more commonplace. In a comprehensive review of the role of HuR in breast cancer (Kotta-Loizou et al., 2016), HuR was reported in functional experiments to act at post-transcriptional levels directly to increase expression of 31 individual target genes and to reduce expression of 4. Excitingly, we have identified cryptic miR-19b binding sites adjacent to the HuR binding site in 3 (75%) of the 3'UTRs from the genes that are down-regulated by HuR (present in *WNT5A*, *IGF1R* and *TP63*, but not in *BRCA1*). Furthermore, expression of these 3 genes, but again not *BRCA1*, demonstrated significant inverse expression correlations with both HuR and with miR-19b in breast cancer patients (Fig S10) – observations that are compatible with HuR/miR-19b acting in concert in all these cases. If regulation by a

functional combination of RNA-binding protein and miRNA is indeed a generic regulatory mechanism, this may have substantial implications for our understanding of post-transcriptional regulation, necessitating both experimental analysis of exactly which RNA-binding proteins and miRNAs combine, and a reassessment of bioinformatic prediction for miRNA binding sites to take into account adjacent sites for RNA-binding proteins and seed regions that do not conform to the current paradigm.

## **5 Conclusion**

The data presented herein demonstrate that the P-glycoprotein mRNA transcript is regulated by cooperation between miR-19b and the RNA-binding protein HuR. Our data support of the hypothesis that HuR allows miR-19b to regulate protein expression through tethering to a non-canonical seed region thus widening its repertoire of binding sites. Whether such non-canonical regulation is a feature specific to the miR19b-ABCB1 pair, or if other miRNA-transcript pairs are regulated in this manner remains to be investigated. Future research should explore if tripartite regulatory complexes are formed at other non-canonical seed-regions and if so, miRNA binding prediction should be re-evaluated.

## **6 Acknowledgements**

The Leeds Breast Research Tissue Bank. The results published here are, in part, based upon data generated by The Cancer Genome Atlas managed by the National Cancer Institute and National Human Genome Research Institute. Information about TCGA can be found at <http://cancergenome.nih.gov>. This work was supported by Breast Cancer Research Action Group (JLT, TAH); the British Council (SJ, TAH); and

the Leeds Cancer Research UK centre (LMW, TAH). The quercetin was a gift from Dr Christine Boesch (Leeds School of Food Science and Nutrition).

### **Author contributions**

JLT and TAH conceptualised the study. JLT, LS and MCT performed wet-lab experiments. RAM-S, LMW and JLT performed histopathology analyses. SB, JLH, SJ and JLT performed in silico analyses. TAH supervised the work. All authors contributed to writing the manuscript.

## REFERENCES

- ARCONDEGUY, T., LACAZETTE, E., MILLEVOI, S., PRATS, H. & TOURIOL, C. 2013. VEGF-A mRNA processing, stability and translation: a paradigm for intricate regulation of gene expression at the post-transcriptional level. *Nucleic Acids Res*, 41, 7997-8010.
- ATLAS, T. C. G. 2012. Comprehensive molecular portraits of human breast tumours. *Nature*, 490, 61-70.
- BAO, L., HAZARI, S., MEHRA, S., KAUSHAL, D., MOROZ, K. & DASH, S. 2012. Increased expression of P-glycoprotein and doxorubicin chemoresistance of metastatic breast cancer is regulated by miR-298. *Am J Pathol*, 180, 2490-503.
- BARRY, W. T., KERNAGIS, D. N., DRESSMAN, H. K., GRIFFIS, R. J., HUNTER, J. D., OLSON, J. A., MARKS, J. R., GINSBURG, G. S., MARCOM, P. K., NEVINS, J. R., GERADTS, J. & DATTO, M. B. 2010. Intratumor heterogeneity and precision of microarray-based predictors of breast cancer biology and clinical outcome. *J Clin Oncol*, 28, 2198-206.
- BOYERINAS, B., PARK, S. M., MURMANN, A. E., GWIN, K., MONTAG, A. G., ZILLHARDT, M., HUA, Y. J., LENGYEL, E. & PETER, M. E. 2012. Let-7 modulates acquired resistance of ovarian cancer to Taxanes via IMP-1-mediated stabilization of multidrug resistance 1. *Int J Cancer*, 130, 1787-97.
- CALADO, R. T., FALCAO, R. P., GARCIA, A. B., GABELLINI, S. M., ZAGO, M. A. & FRANCO, R. F. 2002. Influence of functional MDR1 gene polymorphisms on P-glycoprotein activity in CD34+ hematopoietic stem cells. *Haematologica*, 87, 564-8.
- CANCER GENOME ATLAS, N. 2012. Comprehensive molecular portraits of human breast tumours. *Nature*, 490, 61-70.
- CERAMI, E., GAO, J., DOGRUSOZ, U., GROSS, B. E., SUMER, S. O., AKSOY, B. A., JACOBSEN, A., BYRNE, C. J., HEUER, M. L., LARSSON, E., ANTIPIN, Y., REVA, B., GOLDBERG, A. P., SANDER, C. & SCHULTZ, N. 2012. The cBio cancer genomics portal: an open platform for exploring multidimensional cancer genomics data. *Cancer Discov*, 2, 401-4.
- CHAE, M. J., SUNG, H. Y., KIM, E. H., LEE, M., KWAK, H., CHAE, C. H., KIM, S. & PARK, W. Y. 2009. Chemical inhibitors destabilize HuR binding to the AU-rich element of TNF-alpha mRNA. *Exp Mol Med*, 41, 824-31.
- CHEN, C. J., CLARK, D., UEDA, K., PASTAN, I., GOTTESMAN, M. M. & RONINSON, I. B. 1990. Genomic organization of the human multidrug resistance (MDR1) gene and origin of P-glycoproteins. *J Biol Chem*, 265, 506-14.
- CHU, P. C., KULP, S. K. & CHEN, C. S. 2013. Insulin-like growth factor-I receptor is suppressed through transcriptional repression and mRNA destabilization by a novel energy restriction-mimetic agent. *Carcinogenesis*, 34, 2694-2705.
- CROWLEY, E., MCDEVITT, C. A. & CALLAGHAN, R. 2010. Generating inhibitors of P-glycoprotein: where to, now? *Methods Mol Biol*, 596, 405-32.
- DENKERT, C., WEICHERT, W., WINZER, K. J., MULLER, B. M., NOSKE, A., NIESPOREK, S., KRISTIANSEN, G., GUSKI, H., DIETEL, M. & HAUPTMANN, S. 2004. Expression of the ELAV-like protein HuR is associated with higher tumor grade and increased cyclooxygenase-2 expression in human breast carcinoma. *Clin Cancer Res*, 10, 5580-6.

- DI GIAMMARTINO, D. C., NISHIDA, K. & MANLEY, J. L. 2011. Mechanisms and consequences of alternative polyadenylation. *Mol Cell*, 43, 853-66.
- FAN, X. C. & STEITZ, J. A. 1998. Overexpression of HuR, a nuclear-cytoplasmic shuttling protein, increases the in vivo stability of ARE-containing mRNAs. *EMBO J*, 17, 3448-60.
- FISCHER, S., HANDRICK, R., ASCHRAFI, A. & OTTE, K. 2015. Unveiling the principle of microRNA-mediated redundancy in cellular pathway regulation. *RNA Biol*, 12, 238-47.
- FLAMAND, M. N., GAN, H. H., MAYYA, V. K., GUNSALUS, K. C. & DUCHAINE, T. F. 2017. A non-canonical site reveals the cooperative mechanisms of microRNA-mediated silencing. *Nucleic Acids Res*.
- GAO, J., AKSOY, B. A., DOGRUSOZ, U., DRESDNER, G., GROSS, B., SUMER, S. O., SUN, Y., JACOBSEN, A., SINHA, R., LARSSON, E., CERAMI, E., SANDER, C. & SCHULTZ, N. 2013. Integrative analysis of complex cancer genomics and clinical profiles using the cBioPortal. *Sci Signal*, 6, p11.
- GRIFFITHS-JONES, S. 2004. The microRNA Registry. *Nucleic Acids Res*, 32, D109-11.
- GRIFFITHS-JONES, S., SAINI, H. K., VAN DONGEN, S. & ENRIGHT, A. J. 2008. miRBase: tools for microRNA genomics. *Nucleic Acids Res*, 36, D154-8.
- GRIMSON, A., FARH, K. K., JOHNSTON, W. K., GARRETT-ENGELE, P., LIM, L. P. & BARTEL, D. P. 2007. MicroRNA targeting specificity in mammals: determinants beyond seed pairing. *Mol Cell*, 27, 91-105.
- HAMMOND, S. M., BERNSTEIN, E., BEACH, D. & HANNON, G. J. 2000. An RNA-directed nuclease mediates post-transcriptional gene silencing in *Drosophila* cells. *Nature*, 404, 293-6.
- HE, L. 2010. Posttranscriptional regulation of PTEN dosage by noncoding RNAs. *Sci Signal*, 3, pe39.
- HSU, S. I., COHEN, D., KIRSCHNER, L. S., LOTHSTEIN, L., HARTSTEIN, M. & HORWITZ, S. B. 1990. Structural analysis of the mouse *mdr1a* (P-glycoprotein) promoter reveals the basis for differential transcript heterogeneity in multidrug-resistant J774.2 cells. *Mol Cell Biol*, 10, 3596-606.
- HUANG, Y. H., PENG, W., FURUUCHI, N., GERHART, J., RHODES, K., MUKHERJEE, N., JIMBO, M., GONYE, G. E., BRODY, J. R., GETTS, R. C. & SAWICKI, J. A. 2016. Delivery of Therapeutics Targeting the mRNA-Binding Protein HuR Using 3DNA Nanocarriers Suppresses Ovarian Tumor Growth. *Cancer Res*, 76, 1549-59.
- HUGHES, T. A. 2006. Regulation of gene expression by alternative untranslated regions. *Trends Genet*, 22, 119-22.
- HUNG, C. L., YEN, C. S., TSAI, H. W., SU, Y. C. & YEN, C. J. 2015. Upregulation of MicroRNA-19b predicts good prognosis in patients with hepatocellular carcinoma presenting with vascular invasion or multifocal disease. *BMC Cancer*, 15, 665.
- JIN, H. Y., ODA, H., LAI, M., SKALSKY, R. L., BETHEL, K., SHEPHERD, J., KANG, S. G., LIU, W. H., SABOURI-GHOMI, M., CULLEN, B. R., RAJEWSKY, K. & XIAO, C. 2013. MicroRNA-17~92 plays a causative role in lymphomagenesis by coordinating multiple oncogenic pathways. *EMBO J*, 32, 2377-91.

- KERTESZ, M., IOVINO, N., UNNERSTALL, U., GAUL, U. & SEGAL, E. 2007. The role of site accessibility in microRNA target recognition. *Nat Genet*, 39, 1278-84.
- KIM, B., FATAYER, H., HANBY, A. M., HORGAN, K., PERRY, S. L., VALLELEY, E. M., VERGHESE, E. T., WILLIAMS, B. J., THORNE, J. L. & HUGHES, T. A. 2013. Neoadjuvant chemotherapy induces expression levels of breast cancer resistance protein that predict disease-free survival in breast cancer. *PLoS One*, 8, e62766.
- KIM, H. H., KUWANO, Y., SRIKANTAN, S., LEE, E. K., MARTINDALE, J. L. & GOROSPE, M. 2009. HuR recruits let-7/RISC to repress c-Myc expression. *Genes Dev*, 23, 1743-8.
- KOTTA-LOIZOU, I., VASILOPOULOS, S. N., COUTTS, R. H. & THEOCHARIS, S. 2016. Current Evidence and Future Perspectives on HuR and Breast Cancer Development, Prognosis, and Treatment. *Neoplasia*, 18, 674-688.
- KOVALCHUK, O., FILKOWSKI, J., MESERVY, J., ILNYTSKYI, Y., TRYNDYAK, V. P., CHEKHUN, V. F. & POGRIBNY, I. P. 2008. Involvement of microRNA-451 in resistance of the MCF-7 breast cancer cells to chemotherapeutic drug doxorubicin. *Mol Cancer Ther*, 7, 2152-9.
- LANDGRAF, P., RUSU, M., SHERIDAN, R., SEWER, A., IOVINO, N., ARAVIN, A., PFEFFER, S., RICE, A., KAMPHORST, A. O., LANDTHALER, M., LIN, C., SOCCI, N. D., HERMIDA, L., FULCI, V., CHIARETTI, S., FOA, R., SCHLIWKA, J., FUCHS, U., NOVOSEL, A., MULLER, R. U., SCHERMER, B., BISSELS, U., INMAN, J., PHAN, Q., CHIEN, M., WEIR, D. B., CHOKSI, R., DE VITA, G., FREZZETTI, D., TROMPETER, H. I., HORNUNG, V., TENG, G., HARTMANN, G., PALKOVITS, M., DI LAURO, R., WERNET, P., MACINO, G., ROGLER, C. E., NAGLE, J. W., JU, J., PAPAVALIOU, F. N., BENZING, T., LICHTER, P., TAM, W., BROWNSTEIN, M. J., BOSIO, A., BORKHARDT, A., RUSSO, J. J., SANDER, C., ZAVOLAN, M. & TUSCHL, T. 2007. A mammalian microRNA expression atlas based on small RNA library sequencing. *Cell*, 129, 1401-14.
- LEBEDEVA, S., JENS, M., THEIL, K., SCHWANHAUSSER, B., SELBACH, M., LANDTHALER, M. & RAJEWSKY, N. 2011. Transcriptome-wide analysis of regulatory interactions of the RNA-binding protein HuR. *Mol Cell*, 43, 340-52.
- LI, R. K., GAO, J., GUO, L. H., HUANG, G. Q. & LUO, W. H. 2017. PTENP1 acts as a ceRNA to regulate PTEN by sponging miR-19b and explores the biological role of PTENP1 in breast cancer. *Cancer Gene Ther*, 24, 309-315.
- LI, X., XIE, W., XIE, C., HUANG, C., ZHU, J., LIANG, Z., DENG, F., ZHU, M., ZHU, W., WU, R., WU, J., GENG, S. & ZHONG, C. 2014. Curcumin modulates miR-19/PTEN/AKT/p53 axis to suppress bisphenol A-induced MCF-7 breast cancer cell proliferation. *Phytother Res*, 28, 1553-60.
- LIU, M., YANG, R., URREHMAN, U., YE, C., YAN, X., CUI, S., HONG, Y., GU, Y., LIU, Y., ZHAO, C., YAN, L., ZHANG, C. Y., LIANG, H. & CHEN, X. 2016. MiR-19b suppresses PTPRG to promote breast tumorigenesis. *Oncotarget*, 7, 64100-64108.
- LOPEZ DE SILANES, I., ZHAN, M., LAL, A., YANG, X. & GOROSPE, M. 2004. Identification of a target RNA motif for RNA-binding protein HuR. *Proc Natl Acad Sci U S A*, 101, 2987-92.
- LU, Y. C., CHANG, S. H., HAFNER, M., LI, X., TUSCHL, T., ELEMENTO, O. & HLA, T. 2014. ELAVL1 modulates transcriptome-wide miRNA binding in murine macrophages. *Cell Rep*, 9, 2330-43.

- MARKHAM, N. R. & ZUKER, M. 2008. UNAFold: software for nucleic acid folding and hybridization. *Methods Mol Biol*, 453, 3-31.
- MECHETNER, E., KYSHTOOBAYEVA, A., ZONIS, S., KIM, H., STROUP, R., GARCIA, R., PARKER, R. J. & FRUEHAUF, J. P. 1998. Levels of multidrug resistance (MDR1) P-glycoprotein expression by human breast cancer correlate with in vitro resistance to taxol and doxorubicin. *Clin Cancer Res*, 4, 389-98.
- MECHETNER, E. B. & RONINSON, I. B. 1992. Efficient inhibition of P-glycoprotein-mediated multidrug resistance with a monoclonal antibody. *Proc Natl Acad Sci U S A*, 89, 5824-8.
- MOGILYANSKY, E., CLARK, P., QUANN, K., ZHOU, H., LONDIN, E., JING, Y. & RIGOUTSOS, I. 2016. Post-transcriptional Regulation of BRCA2 through Interactions with miR-19a and miR-19b. *Front Genet*, 7, 143.
- MUKHERJEE, N., CORCORAN, D. L., NUSBAUM, J. D., REID, D. W., GEORGIEV, S., HAFNER, M., ASCANO, M., JR., TUSCHL, T., OHLER, U. & KEENE, J. D. 2011. Integrative regulatory mapping indicates that the RNA-binding protein HuR couples pre-mRNA processing and mRNA stability. *Mol Cell*, 43, 327-39.
- MURALIDHARAN, R., MEHTA, M., AHMED, R., ROY, S., XU, L., AUBE, J., CHEN, A., ZHAO, Y. D., HERMAN, T., RAMESH, R. & MUNSHI, A. 2017. HuR-targeted small molecule inhibitor exhibits cytotoxicity towards human lung cancer cells. *Sci Rep*, 7, 9694.
- OLIVE, V., BENNETT, M. J., WALKER, J. C., MA, C., JIANG, I., CORDON-CARDO, C., LI, Q. J., LOWE, S. W., HANNON, G. J. & HE, L. 2009. miR-19 is a key oncogenic component of mir-17-92. *Genes Dev*, 23, 2839-49.
- OTTMAN, R., LEVY, J., GRIZZLE, W. E. & CHAKRABARTI, R. 2016. The other face of miR-17-92a cluster, exhibiting tumor suppressor effects in prostate cancer. *Oncotarget*, 7, 73739-73753.
- PATEL, N., GARIKAPATI, K. R., PANDITA, R. K., SINGH, D. K., PANDITA, T. K., BHADRA, U. & BHADRA, M. P. 2017. miR-15a/miR-16 down-regulates BMI1, impacting Ub-H2A mediated DNA repair and breast cancer cell sensitivity to doxorubicin. *Sci Rep*, 7, 4263.
- PENG, S. S., CHEN, C. Y., XU, N. & SHYU, A. B. 1998. RNA stabilization by the AU-rich element binding protein, HuR, an ELAV protein. *Embo J*, 17, 3461-70.
- PORIA, D. K., GUHA, A., NANDI, I. & RAY, P. S. 2016. RNA-binding protein HuR sequesters microRNA-21 to prevent translation repression of proinflammatory tumor suppressor gene programmed cell death 4. *Oncogene*, 35, 1703-1715.
- POUPON, R., PING, C., CHRETIEN, Y., CORPECHOT, C., CHAZOUILLERES, O., SIMON, T., HEATH, S. C., MATSUDA, F., POUPON, R. E., HOUSSET, C. & BARBU, V. 2008. Genetic factors of susceptibility and of severity in primary biliary cirrhosis. *J Hepatol*, 49, 1038-45.
- RAGUZ, S., RANDLE, R. A., SHARPE, E. R., FOEKENS, J. A., SIEUWERTS, A. M., MEIJER-VAN GELDER, M. E., MELO, J. V., HIGGINS, C. F. & YAGUE, E. 2008. Production of P-glycoprotein from the MDR1 upstream promoter is insufficient to affect the response to first-line chemotherapy in advanced breast cancer. *Int J Cancer*, 122, 1058-67.
- RANDLE, R. A., RAGUZ, S., HIGGINS, C. F. & YAGUE, E. 2007. Role of the highly structured 5'-end region of MDR1 mRNA in P-glycoprotein expression. *Biochem J*, 406, 445-55.

- SATHEESHA, S., COOKSON, V. J., COLEMAN, L. J., INGRAM, N., MADHOK, B., HANBY, A. M., SULEMAN, C. A. B., SABINE, V. S., MACASKILL, E. J., BARTLETT, J. M. S., DIXON, J. M., MCELWAINE, J. N. & HUGHES, T. A. 2011. Response to mTOR inhibition: activity of eIF4E predicts sensitivity in cell lines and acquired changes in eIF4E regulation in breast cancer. *Molecular Cancer*, 10.
- SMITH, L., BAXTER, E. W., CHAMBERS, P. A., GREEN, C. A., HANBY, A. M., HUGHES, T. A., NASH, C. E., MILLICAN-SLATER, R. A., STEAD, L. F., VERGHESE, E. T. & SPEIRS, V. 2015. Down-Regulation of miR-92 in Breast Epithelial Cells and in Normal but Not Tumour Fibroblasts Contributes to Breast Carcinogenesis. *Plos One*, 10.
- SMITH, L., BRANNAN, R. A., HANBY, A. M., SHAABAN, A. M., VERGHESE, E. T., PETER, M. B., POLLOCK, S., SATHEESHA, S., SZYNKIEWICZ, M., SPEIRS, V. & HUGHES, T. A. 2010a. Differential regulation of oestrogen receptor beta isoforms by 5' untranslated regions in cancer. *J Cell Mol Med*, 14, 2172-84.
- SMITH, L., COLEMAN, L. J., CUMMINGS, M., SATHEESHA, S., SHAW, S. O., SPEIRS, V. & HUGHES, T. A. 2010b. Expression of oestrogen receptor beta isoforms is regulated by transcriptional and post-transcriptional mechanisms. *Biochem J*, 429, 283-90.
- TANABE, M., IEIRI, I., NAGATA, N., INOUE, K., ITO, S., KANAMORI, Y., TAKAHASHI, M., KURATA, Y., KIGAWA, J., HIGUCHI, S., TERAKAWA, N. & OTSUBO, K. 2001. Expression of P-glycoprotein in human placenta: relation to genetic polymorphism of the multidrug resistance (MDR)-1 gene. *J Pharmacol Exp Ther*, 297, 1137-43.
- TROCK, B. J., LEONESSA, F. & CLARKE, R. 1997. Multidrug resistance in breast cancer: a meta-analysis of MDR1/gp170 expression and its possible functional significance. *J Natl Cancer Inst*, 89, 917-31.
- TULSYAN, S., MITTAL, R. D. & MITTAL, B. 2016. The effect of ABCB1 polymorphisms on the outcome of breast cancer treatment. *Pharmgenomics Pers Med*, 9, 47-58.
- TURTON, N. J., JUDAH, D. J., RILEY, J., DAVIES, R., LIPSON, D., STYLES, J. A., SMITH, A. G. & GANT, T. W. 2001. Gene expression and amplification in breast carcinoma cells with intrinsic and acquired doxorubicin resistance. *Oncogene*, 20, 1300-6.
- UEDA, K., CLARK, D. P., CHEN, C. J., RONINSON, I. B., GOTTESMAN, M. M. & PASTAN, I. 1987. The human multidrug resistance (mdr1) gene. cDNA cloning and transcription initiation. *J Biol Chem*, 262, 505-8.
- VACLAVIKOVA, R., EHRlichOVA, M., HlavATA, I., PECHA, V., KOZEVNIKOVova, R., TRNKOVA, M., ADAMEK, J., EDVARDSEN, H., KRISTENSEN, V. N., GUT, I. & SOUCEK, P. 2012. Detection of frequent ABCB1 polymorphisms by high-resolution melting curve analysis and their effect on breast carcinoma prognosis. *Clin Chem Lab Med*, 50, 1999-2007.
- VALLEJO, D. M., CAPARROS, E. & DOMINGUEZ, M. 2011. Targeting Notch signalling by the conserved miR-8/200 microRNA family in development and cancer cells. *EMBO J*, 30, 756-69.
- VAN NES, J. G., DE KRUIJF, E. M., PUTTER, H., FARATIAN, D., MUNRO, A., CAMPBELL, F., SMIT, V. T., LIEFERS, G. J., KUPPEN, P. J., VAN DE VELDE, C. J. & BARTLETT, J. M. 2012. Co-expression of SNAIL and TWIST determines prognosis in estrogen receptor-positive early breast cancer patients. *Breast Cancer Res Treat*, 133, 49-59.

- VERGHESE, E. T., DRURY, R., GREEN, C. A., HOLLIDAY, D. L., LU, X., NASH, C., SPEIRS, V., THORNE, J. L., THYGESEN, H. H., ZOUGMAN, A., HULL, M. A., HANBY, A. M. & HUGHES, T. A. 2013. MiR-26b is down-regulated in carcinoma-associated fibroblasts from ER-positive breast cancers leading to enhanced cell migration and invasion. *J Pathol*, 231, 388-99.
- WANG, J., GUO, Y., CHU, H., GUAN, Y., BI, J. & WANG, B. 2013. Multiple functions of the RNA-binding protein HuR in cancer progression, treatment responses and prognosis. *Int J Mol Sci*, 14, 10015-41.
- WIGHTMAN, B., HA, I. & RUVKUN, G. 1993. Posttranscriptional regulation of the heterochronic gene *lin-14* by *lin-4* mediates temporal pattern formation in *C. elegans*. *Cell*, 75, 855-62.
- WU, X., LAN, L., WILSON, D. M., MARQUEZ, R. T., TSAO, W. C., GAO, P., ROY, A., TURNER, B. A., MCDONALD, P., TUNGE, J. A., ROGERS, S. A., DIXON, D. A., AUBE, J. & XU, L. 2015. Identification and validation of novel small molecule disruptors of HuR-mRNA interaction. *ACS Chem Biol*, 10, 1476-84.
- YAMAGUCHI, H., HISHINUMA, T., ENDO, N., TSUKAMOTO, H., KISHIKAWA, Y., SATO, M., MURAI, Y., HIRATSUKA, M., ITO, K., OKAMURA, C., YAEGASHI, N., SUZUKI, N., TOMIOKA, Y. & GOTO, J. 2006. Genetic variation in ABCB1 influences paclitaxel pharmacokinetics in Japanese patients with ovarian cancer. *Int J Gynecol Cancer*, 16, 979-85.
- ZHU, X. Z., ZELMER, A., KAPFHAMMER, J. P. & WELLMANN, S. 2016. Cold-inducible RBM3 inhibits PERK phosphorylation through cooperation with NF90 to protect cells from endoplasmic reticulum stress. *Faseb Journal*, 30, 624-634.
- ZHU, Z., WANG, B., BI, J., ZHANG, C., GUO, Y., CHU, H., LIANG, X., ZHONG, C. & WANG, J. 2013. Cytoplasmic HuR expression correlates with P-gp, HER-2 positivity, and poor outcome in breast cancer. *Tumour Biol*, 34, 2299-308.

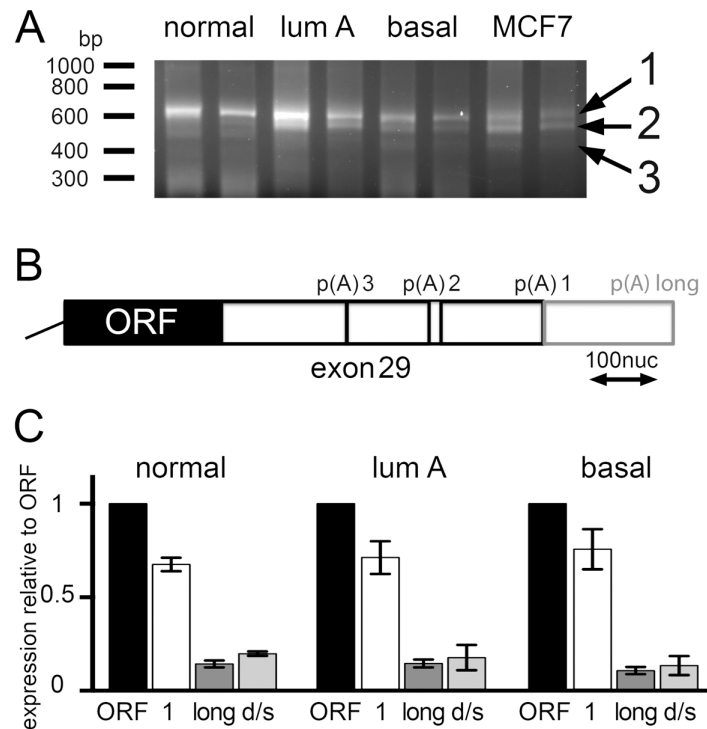


**Fig 1. Breast epithelial cells express three alternative *ABCB1* 3'UTRs.** **A)** 3'RACE for *ABCB1* was performed on RNA from normal breast tissue, a luminal A tumour, a basal-like tumour, and MCF7 cells as shown. An agarose gel is shown with RACE products from samples as labelled, loaded into two lanes each. The numbers demark three major RACE products, representing 3'UTRs of 384 (1), 252-259 (2), and 119 bases (3). **B)** RACE products were sequenced and analysed to align with genomic DNA. A scaled schematic showing the positions of poly(A) sites 1, 2 and 3 that produce the same numbered different UTR lengths. Also illustrated in grey is the longer 3'UTR previously reported (Bao et al., 2012, Kovalchuk et al., 2008). **C)** Expression relative to the *ABCB1* open reading frame (ORF) was determined by qPCR in the samples as labelled for various actual or potential UTR sequences. 1 represents sequences terminating at p(A) site 1, 'long' represents the longer 3'UTR sequence previously studied, and d/s represents background expression of a sequence >5kb downstream of the gene. Mean of three biological replicates with SEM are displayed.

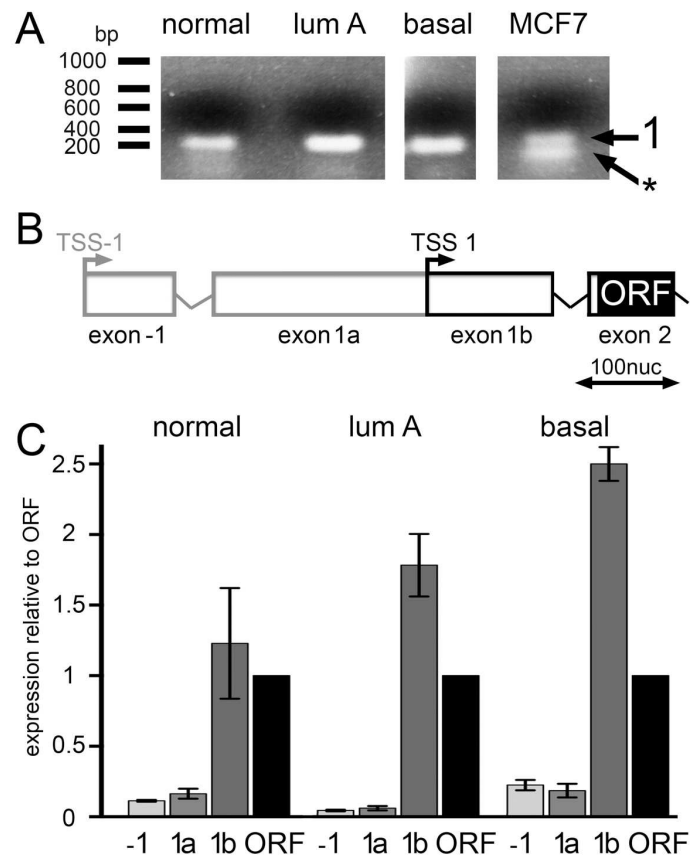


**Fig 2. Breast epithelial cells express one *ABCB1* 5'UTR.** **A)** 5'RACE for *ABCB1* was performed on RNA from normal breast tissue, a luminal A tumour, a basal-like tumour, and MCF7 cells as shown. An agarose gel is shown with RACE products as labelled. 1 denotes the only specific product representing a 5'UTR of 132-134 bases, while \* denotes a non-specific product. **B)** RACE products were sequenced and analysed to align with genomic DNA. A schematic is shown demonstrating how the UTR identified maps onto exon structure. Also illustrated in grey is the previously reported upstream exon structure. Alternative transcription start sites (TSS) are indicated. **C)** Expression relative to the *ABCB1* open reading frame (ORF) was determined by qPCR in the samples as labelled for various actual or potential UTR sequences. Sequences from exon -1, 1a and 1b were tested. Mean of three biological replicates with SEM are displayed.

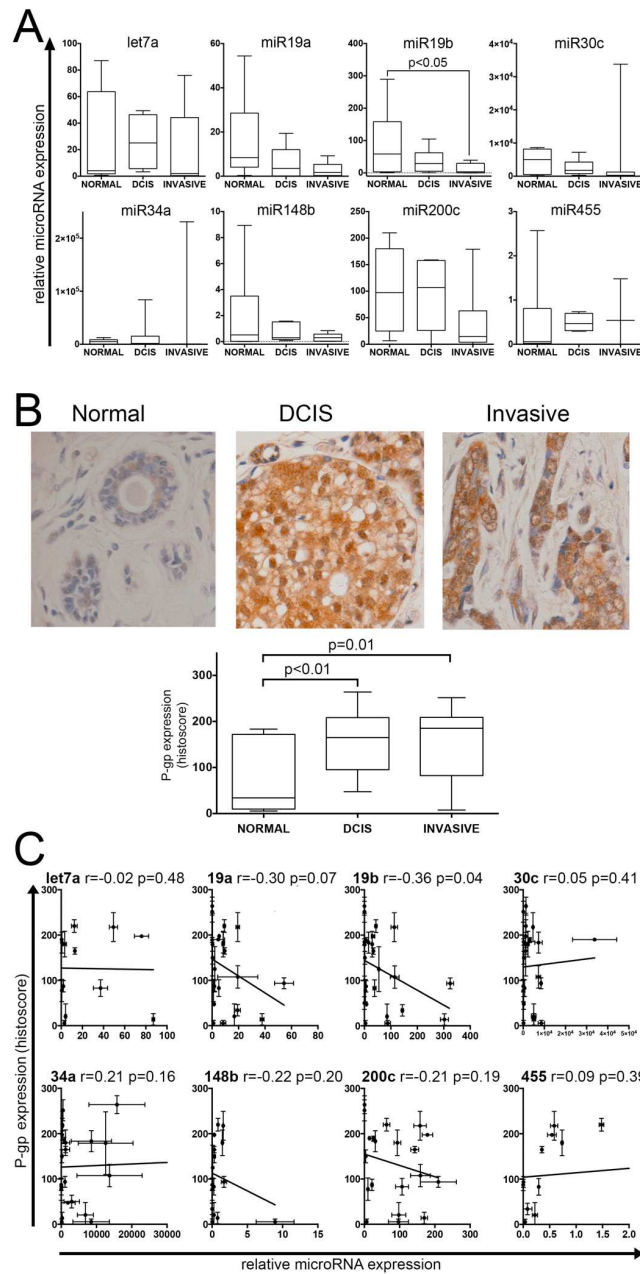


**Fig 3. Expression of P-gp, the protein product of *ABCB1*, is inversely correlated with expression of miR-19b.** **A)** Laser microdissection of epithelial cells from 9 breast cancer cases with matched samples of normal epithelium, ductal carcinoma in situ (DCIS), and invasive cancer was performed. Expression of miRNAs as labelled was assessed by qPCR. Boxes show 25<sup>th</sup>-75<sup>th</sup> percentiles, whiskers show range and median is shown as the line (Wilcoxon matched-pairs rank test two-tailed). **B)** The same tissues were stained for P-gp expression by immunohistochemistry and expression within epithelial cells was quantified as histoscores. Representative immunohistochemistry images (top) and P-gp histoscore (bottom). Whiskers show range and median is shown as the line (Wilcoxon matched-pairs rank test two-tailed). **C)** MiRNA expression and P-gp histoscores were paired for every sample and tested for correlation (Spearman's rank, coefficient,  $r$ , and significance,  $p$ ).

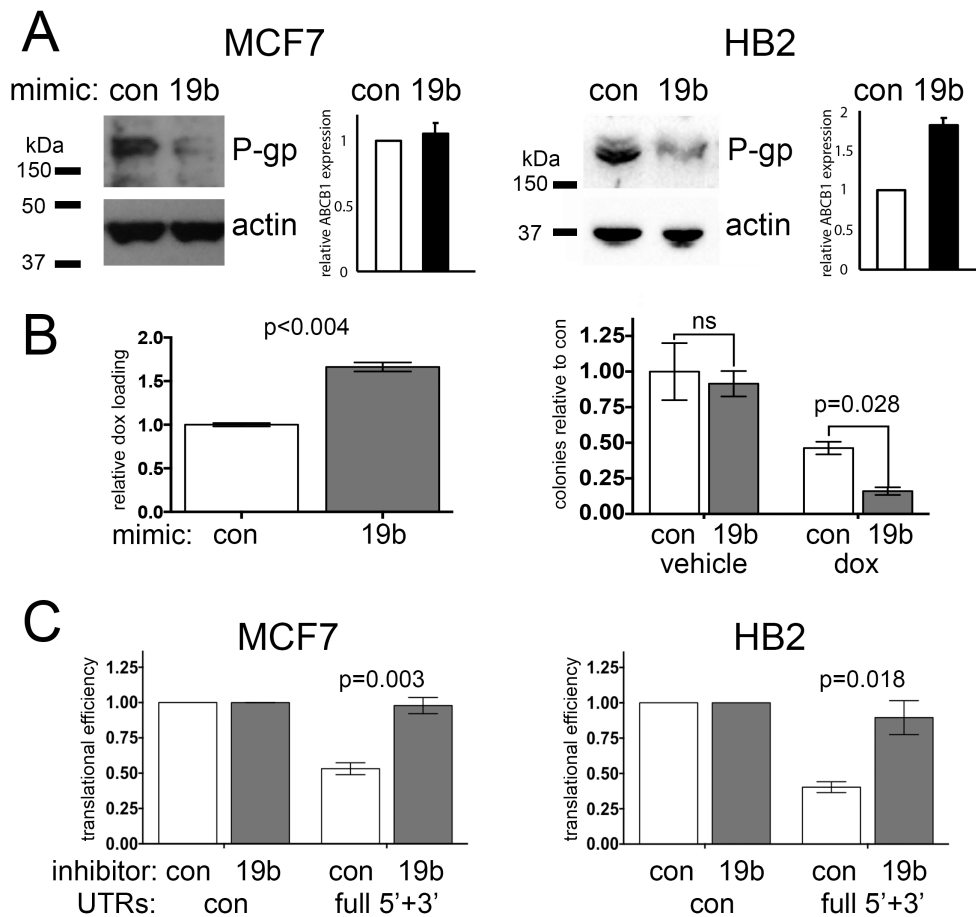


**Fig 4. MiR-19b directly suppresses P-gp translation and enhances doxorubicin mediated cell death.** MCF7 or HB2 cells, as labelled, were transiently transfected with miR-19b mimics, inhibitors or appropriate controls, or with luciferase reporters as shown. **A)** Western Blots showing P-gp expression (and expression of a loading control) after 48h after transfection with miR-19b mimic or control. Blots are representative of 2 biological repeats. qPCR analysis showing relative expression of ABCB1 after the same transfections. Data represent means (+/- SEM) of 2 biological repeats. **B)** MCF7 cells were transfected with miR-19b mimic or control, and 24h later were treated with 10 nM doxorubicin for 24h. Intra-cellular loading with doxorubicin was measured by flow-cytometry (left), while survival was assessed in colony forming assays (right). **C)** Plasmids were cloned to allow expression of GFP transcripts flanked by control non-specialised UTRs (con) or the 5' and 3' UTRs identified as expressed in breast cells on *ABCB1* transcripts (full 5'+3'). Cells were transfected with plasmids and miR-19b inhibitor or inhibitor control and translation efficiency (GFP protein produced relative to GFP transcript) was assessed using flow-cytometry and qPCR. Mean of at least 3-5 biological replicates with SEM is presented. Two-tailed Student's t-test was performed.

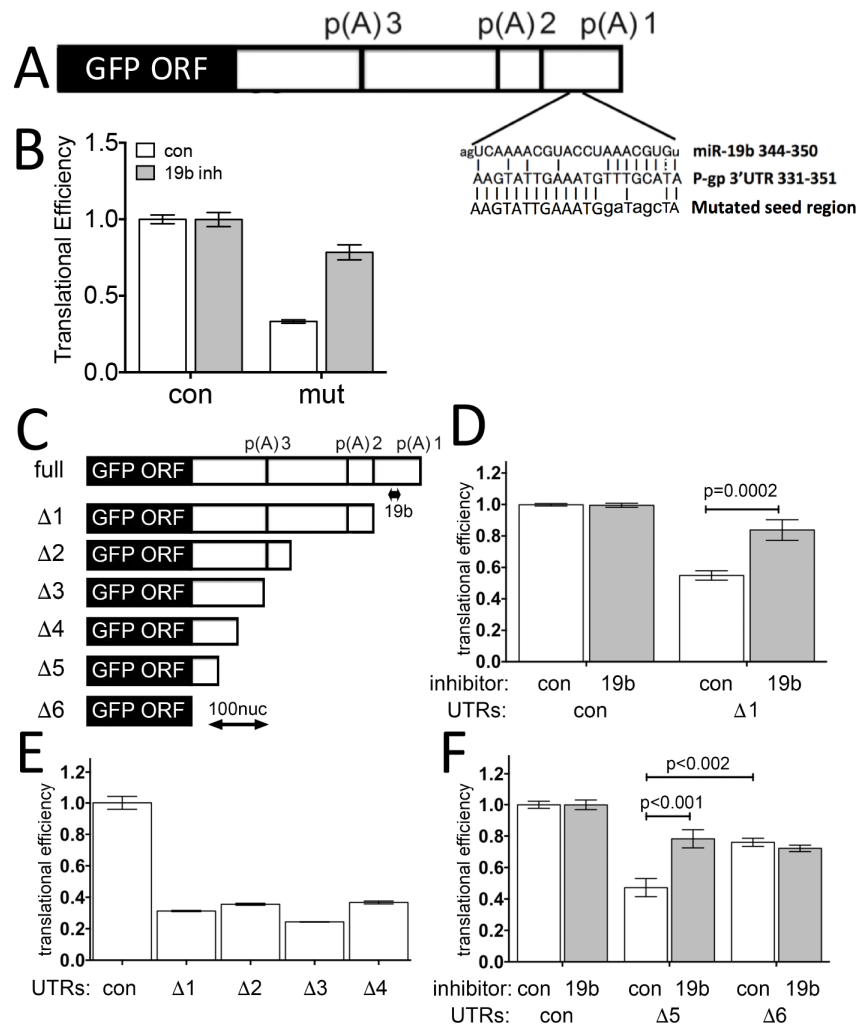


**Fig 5. MiR-19b response of the ABCB1 3'UTR requires sequences adjacent to the reading frame, while the more distal canonical miR-19b site is superfluous.**

A) Schematic of the ABCB1 3'UTR showing positions of the 3 alternative polyadenylation sites [p(A) 1, 2 and 3], and the canonical miR-19b binding site. Mutations introduced in the binding site in reporter assays in (B) are shown in lower case. B) The predicted miR-19 binding site was mutated, as shown in (A), in the context of the full 5'+3' reporter. MCF7 cells were transfected with either the control, non-specialised reporter (con) or the mutated full 5'+3' reporter (mut) along miR-19b inhibitor (19b inh) or inhibitor control (con). Translation efficiency was assessed using flow-cytometry and qPCR. C) A schematic showing the series of GFP reporters expressing ABCB1 3'UTRs with progressively larger deletions. The position of the canonical miR-19b binding site is shown on the "full" sequence. D-F) MCF7 cells were transfected with either the control, non-specialised reporter (con) or the ABCB1 UTR reporter indicated, along with miR-19b inhibitor or inhibitor control (D and F only). Translation efficiency was determined. All bars show mean of 2-4 biological replicates with SEM. Two-tailed Student's t-tests were applied.

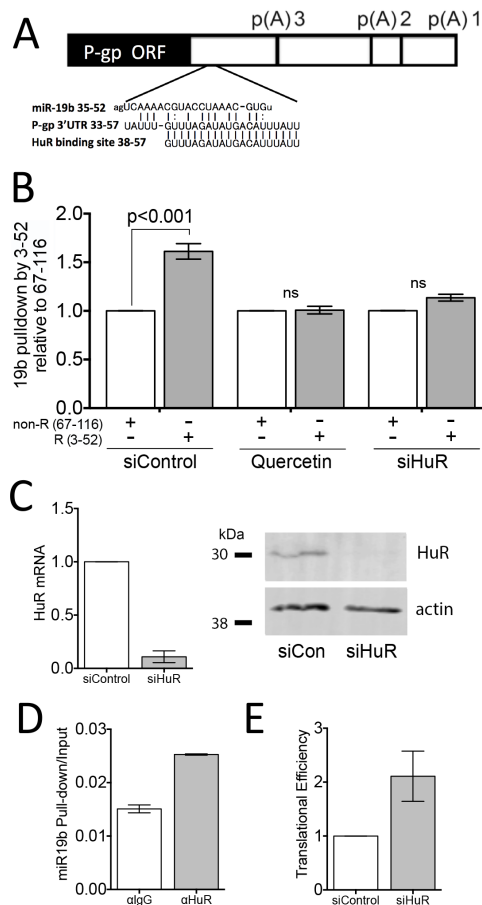


**Fig 6. MiR-19b association with the ABCB1 3'UTR is dependent on HuR.** A) Schematic of the ABCB1 3'UTR showing positions of a potential binding site for miR-19b, which does not conform to any consensus, and a consensus binding site for the RNA-binding protein HuR. Numbers denote base position relative to start of UTR. B) Biotinylated oligos corresponding to either the miR-19b responsive region (R; bases 3-52 of the 3'UTR), or the adjacent non-responsive region (non-R; bases 67-116) were used in a pull-down assay with nuclear lysates from MCF7 cells that had been either transfected with siRNA against HuR or control siRNA, or treated with the chemical inhibition of HuR, quercetin (10 $\mu$ M). Recovery of miR-19b was assessed by qPCR. C) MCF7 cells were transfected with siRNA against HuR or control siRNA and expression of HuR was assessed using qPCR and Western blot. D) Immunoprecipitations were performed from nuclear lysates of MCF7 cells using an antibody directed against HuR, or an isotope control antibody. Recovery of miR-19b was assessed by qPCR. E) MCF7 cells were transfected with the minimal miR-19b-responsive ABCB1 UTR reporter ( $\Delta$ 5), along with siRNA against HuR or control siRNA. Translation efficiency was assessed using flow-cytometry and qPCR. (D) and (E) show mean and SD of two technical replicates. (B) and (C) show mean and SEM of two biological replicates.

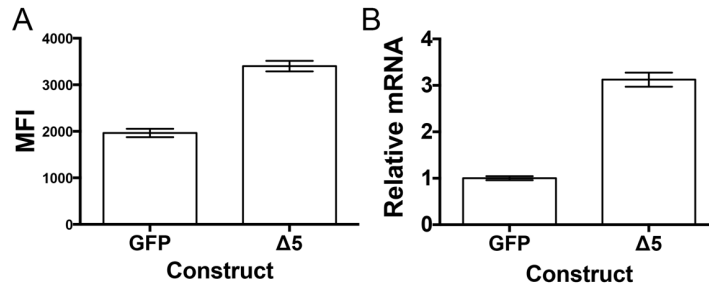


**Fig S1 Representative data showing quantification of GFP protein and transcript for assessment of translational efficiency.** Flow cytometry was used to quantify Mean Fluorescence Intensity (GFP protein expression; A) and qPCR to quantify relative GFP transcript expression (B). These were used to calculate translational efficiency (protein per unit transcript). Data shown represent means of technical replicates (+/- SD) for one biological experiment comparing translational efficiency of the GFP control construct with the delta 5 deletion mutant (see Fig 5C) in MCF7 cells.

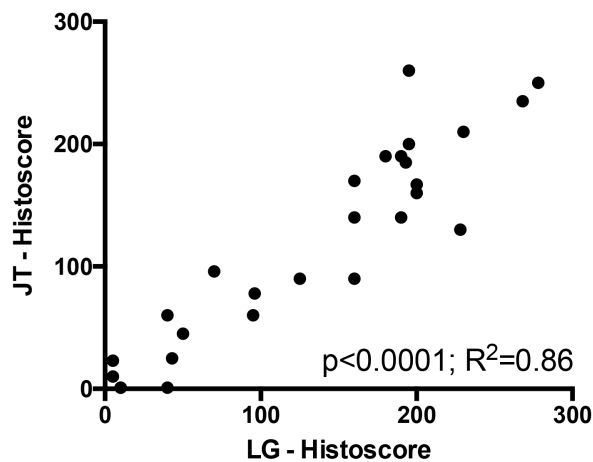


**Fig S2. Interclass correlation between independent observers for scoring of P-gp immunohistochemistry.** Scores given by scorer 1, LW, are plotted against scorer 2, JT. The inter-class correlation was calculated using Pearson's correlation:  $r^2 = 0.86$ ;  $p < 0.0001$ .

rs3213619 (T/C)

↓

```

Ueda      1>CTGAGCTCATTCAGTAGCGGCTCTTCCAAGCTCAAAGAAGCAGAGGCCGCTGTTTCGTTTCCTTTAGGTCCTTCCACTAAAGTCGGAGTATCTTCTTCCA>100
Product 1 1>-----GTAGCGGCTCTTCCAAGCTCAAAGAAGCAGAGGCCGCTGTTTCGTTTCCTTTAGGTCCTTCCACTAAAGTCGGAGTATCTTCTTCCA>86
Product 2 1>-----GAGTAGCGGCTCTTCCAAGCTCAAAGAAGCAGAGGCCGCTGTTTCGTTTCCTTTAGGTCCTTCCACTAAAGTCGGAGTATCTTCTTCCA>88

```

M  
ATG

```

Ueda      101>AAATTTACAGTCTTGGTGGCCGTTCCAAGGAGCGCGAGTCGGAATG>146
Product 1 87>AAATTTACAGTCTTGGTGGCCGTTCCAAGGAGCGCGAGTCGGAATG>132
Product 2 89>AAATTTACAGTCTTGGTGGCCGTTCCAAGGAGCGCGAGTCGGAATG>134

```

↑  
rs2214102 (A/G)

**Fig S3. ABCB1 5'UTR sequences aligned to the previously reported exon 1b-derived sequence.** Two different lengths of 5'UTR products were identified by 5'RACE from breast epithelial cells. These are represented by product 1, and product 2 of 129 or 131 bases respectively. These sequences are aligned to the slightly longer 5'UTR sequence identified in Ueda et al (Ueda et al., 1987). The positions and variants for SNPs rs3213619 and rs2214102 are highlighted (see Fig S5), with the major variant present within the sequence in both locations. The start codon is indicated by additional text ATG and M (for methionine) above the sequences.

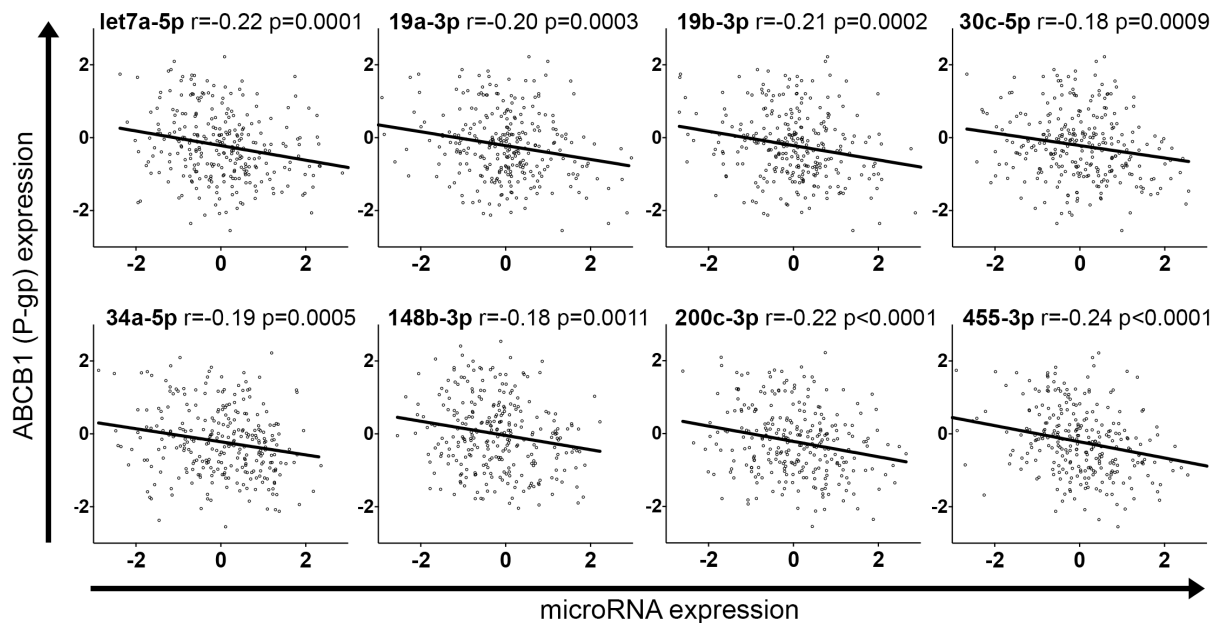


**Fig S4. 8 miRNAs were shortlisted as potential regulators of ABCB1 expression.** Pearson rank correlations were calculated for miRNA expression (x-axis) vs ABCB1 expression (y-axis). Those with significant negative correlations are shown as scatter plots with a linear regression line plotted. Correlation coefficients, r, and significance values, p, are shown.

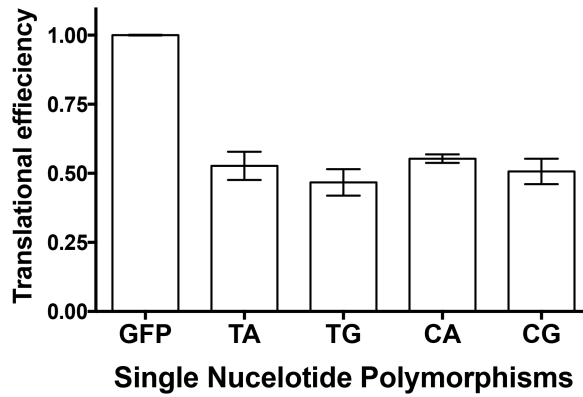


**Fig S5. SNP variants at rs3213619 and rs2214102 within the *ABCB1* 5'UTR do not affect translational efficiency.** SNP variants at rs3213619 and rs2214102 were created in the context of *ABCB1* UTR reporters, as indicated (rs3213619, either T or C in the first position; rs2214102, either A or G, in the second position). MCF7 cells were transfected with either the GFP reporter lacking specialised UTRs (GFP) or *ABCB1* UTR reporters and relative translation efficiency of reporter transcripts was assessed using flow-cytometry and qPCR.

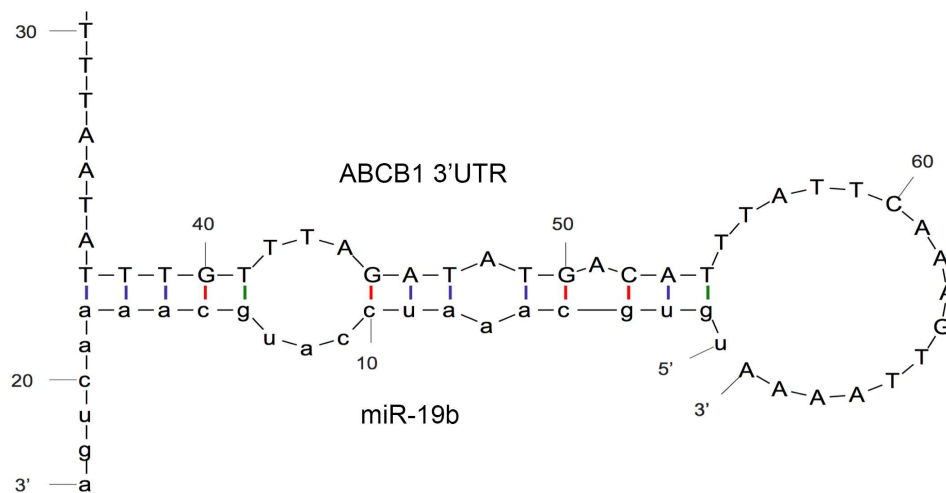


**Fig S6. Predicted base-pairing structure of miR-19b and *ABCB1* non-canonical site.** Bases 30 to 70 of the *ABCB1* 3'UTR and the mature hsa-miR-19b sequence were aligned using the UNAFold two-state hybridization tool (Markham and Zuker, 2008). Binding occurs with free energy of -7.9 kcal/mol.

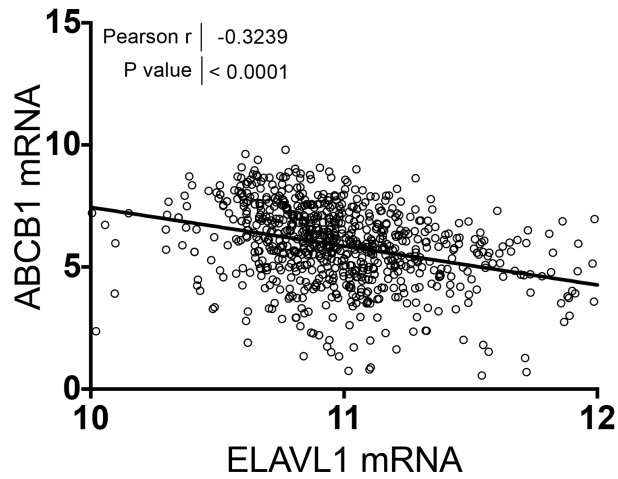


**Fig S7. ABCB1 (P-gp) and ELAV1 (HuR) mRNA expression levels negatively correlate in breast tumours.** Log transformed expression data from previously published TCGA RNA-Seq datasets were downloaded from the Broad Institute's TCGA Firehose site. Data represent 774 breast cancers for which matching mRNA and miRNA-Seq data were available. Data were plotted on a scatter graph, and a Pearson's correlation test was performed.

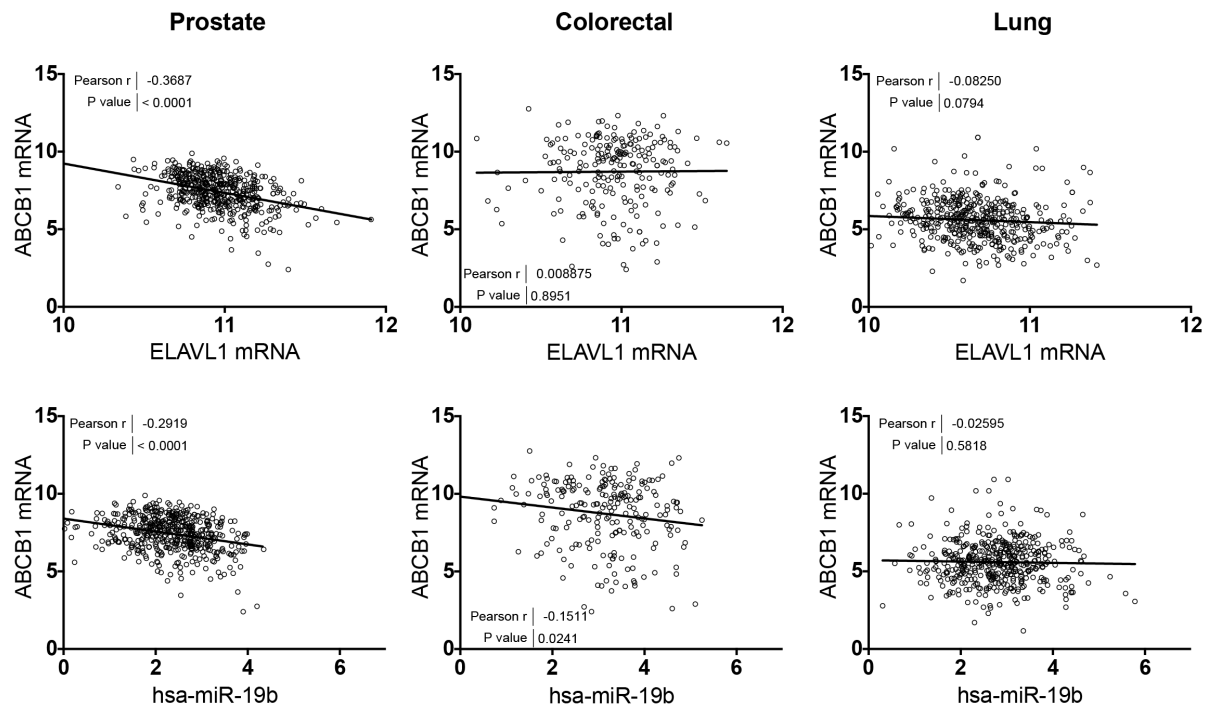


**Fig S8. ABCB1 (P-gp) expression negatively correlates with ELAV1 (HuR) mRNA expression and with miR-19b expression in prostate, but not colorectal or lung tumours.** Log transformed expression data from previously published TCGA RNA-Seq datasets were downloaded from the Broad Institute's TCGA Firehose site. Data represent 496 prostate cancers, 223 colorectal cancers, and 453 lung cancers. Data were plotted on scatter graphs, and Pearson's correlation tests were performed. Pearson's correlation was performed. Correlations in prostate cancers were highly significant ( $p < 0.0001$ ). Correlation between ABCB1 and miR-19b in colorectal cancers was significant at  $p < 0.05$ , but this is excluded using a Bonferroni-corrected target p value of 0.008 to take into account multiple tests.

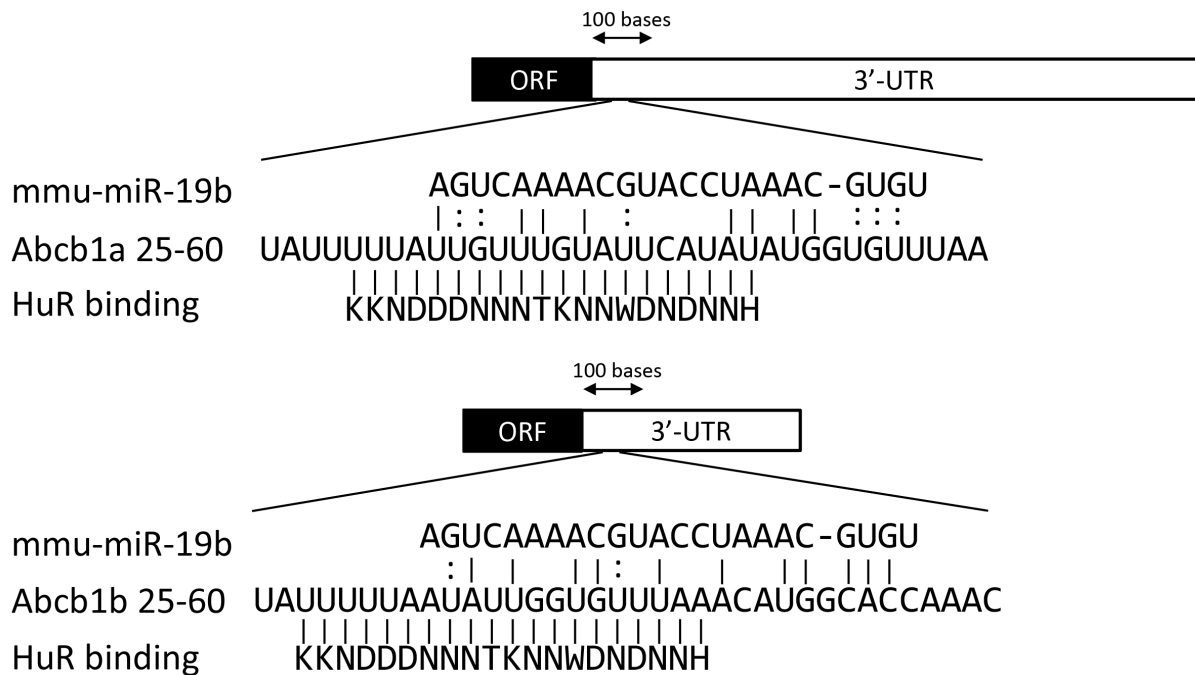


**Fig S9. Overlapping potential miR-19b and HuR binding sites are present in the 3'UTR regions of both murine genes encoding P-gp proteins, *Abcb1a* and *Abcb1b*.** Schematics showing alignments locating, in terms of bases from the start of the 3'UTR, potential binding sites for miR-19b and HuR in the two murine homologues of the human ABCB1 gene.

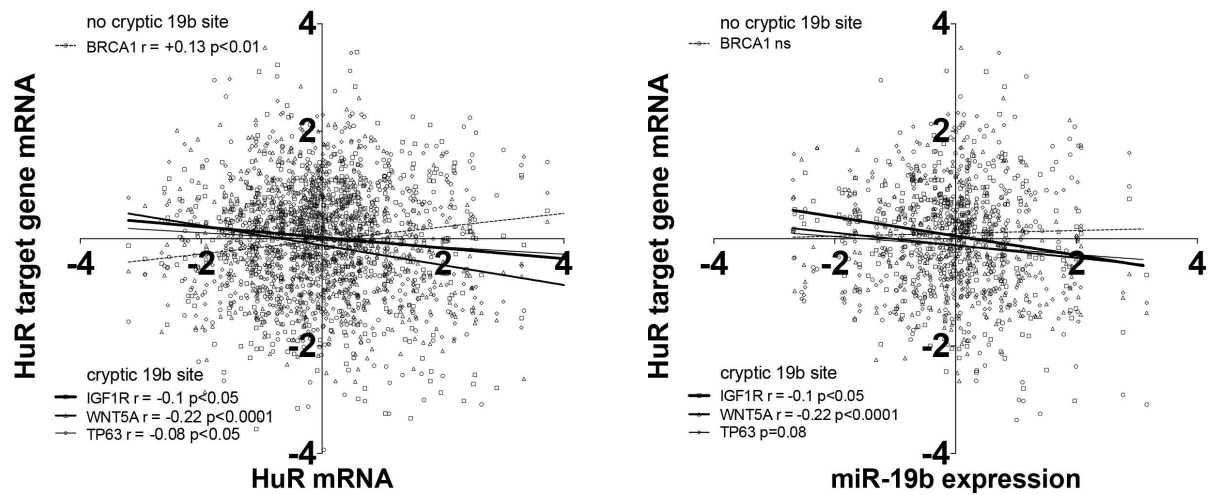


**Fig S10. mRNAs reported to be targets of HuR-mediated repression that contain cryptic miR-19b seed regions adjacent to a HuR binding site are inversely correlated with HuR (A) and miR-19b (B).** Expression data for the mRNAs and miR-19b were downloaded from TCGA and Pearson's rank correlation analyses performed; p values and r values for significant correlations are shown.

	5'-3'
<b>qPCR</b>	
36B4 (+)	GAAACTCTGCATTCTCGCTTCC
36B4 (-)	GATGCAACAGTTGGGTAGCCA
ABCB1 ORF (+)	TGGTTCAGGTGGCTCTGGAT
ABCB1 ORF (-)	CTGTAGACAAACGATGAGCTATCACA
ABCB1 3'UTR 1 (+)	ACATCATCAAGTGGAGAGAAAT
ABCB1 3'UTR 1 (-)	GGCAGTCAGTTACAGTCCAA
ABCB1 3'UTR Bao (+)	tggctctcaaacccaaaacacagatcg
ABCB1 3'UTR Bao (-)	cataattgtgcctcaccacacctcc
ABCB1 3'UTR d/s (+)	gaggtggagcccctcccagg
ABCB1 3'UTR d/s (-)	agcaccctctctgacagcc
HuR (+)	CGAAGCCTGTTTCAGCAGCATTG
HuR (-)	GTTCACAAAGCCATAGCCCAAGC
<b>RACE</b>	
3'RACE +4103 (+)	TGCTGGCACAGAAAGGCATC
5'RACE +5 nested (-)	ATTGCGGTCCCCTTCAAGA
5'RACE -32 RT (-)	CTTGGAACGGCCACCAAGAC
<b>3'UTR cloning/deletions</b>	
ABCB1 3'-UTR (+)	GGATCCACTCTGACTGTATGAGA
ABCB1 3'-UTR full (-)	GCAAGCTTCCAGTCACATGAAAGTTTAG
ABCB1 3'-UTR full d1 (-)	GCAAGCTTTATCTTTTAAAATCTACTTTAATTCTGTT
Forward primer d2-6 (+)	GCTTGGGCCCGAACAAAA
ABCB1 3'-UTR full d2 (-)	TTTAAACTATGATTTCTCTCCACTTG
ABCB1 3'-UTR full d3 (-)	ATTACGAAGTCTCTGAAGACTC
ABCB1 3'-UTR full d4 (-)	ATACCTCTTCATAATTCTGTAAGTGTTG
ABCB1 3'-UTR full d5 (-)	CATATCTAAACAAATATTA AAAAAGTATTTAACATCTC
ABCB1 3'-UTR full d6 (-)	TCTTACTTGTACAGCTCGTC
<b>Sequencing</b>	
5'UTR confirmation	
CMV (+)	CGCAAATGGGCGGTAGGCGTG
EGFP (-)	CTGGTCGAGCTGGACGGCGACG
3'UTR confirmation	
BGH-R (+)	CCTCGACTGTGCCTTCTA
EGFP (-)	CATGGTCCTGCTGGAGTTCGTG
<b>UTR-pulldown assay</b>	
NonR (67-116)	/5Biosg/rArArArGrCrArArArCrArCrUrUrArCrArGrArArUrUrArUrGrArArGrArGrUrArUrCrUrGrUrUrUrArArCrArUrUrUrCrCrU
Res (3-52)	/5Biosg/rCrUrCrUrGrArCrUrGrUrArUrGrArGrArUrGrUrUrArArArUrArCrUrUrUrUrArArUrArUrUrGrUrUrUrArGrArUrArUrG
<b>Site-Directed Mutagenesis of miR-19b seed region</b>	
Q5SDM (+)	gctaAAAGTGTCTATAATAAACTAACTTTC
Q5SDM (-)	tatcaTTTCAATACTTTTGTACTTCTATAAT

**Table S1 Primer and Oligo sequences**

microRNA	Mature Sequence 5' to 3'	Binding Position relative ORF end	Seed	dGduplex	ddG/dGopen
hsa-let-7a-5p	ugagguaguagguuguauaquu	110	8:1:1	-11.3	0.32
hsa-miR-19a-3p	ugugcaaaucuaugcaaaacuga	340	7:0:1	-12.1	0.94
hsa-miR-19b-1-3p	ugugcaaauccaugcaaaacuga	340	7:0:1	-12.1	0.94
hsa-miR-30c-5p	uguaaacauccuacacucucagc	102, 263, 196, 337	7:1:0	-11	0.43
hsa-miR-34a-5p	uggcagugucuuagcugguugu	294, 202, 290	6:0:0	-15.4	1.64
hsa-miR-148b-3p	ucagugcaucacagaacuuugu	204	7:1:1	-9.5	0.36
hsa-miR-200c-3p	uaauacugccggguaaugaugga	328	6:0:0	-9.15	0.67
hsa-miR-455-3p	gcaguccaugggcauauacac	281, 378, 292	7:0:0	-17.7	1.37

**Table S2. MiRNAs predicted to bind the *ABCB1* 3'UTR.** miRNA name and strand are shown in the first column. The mature sequence is given and the first base-pairing site is shown as "position". Position 1 would denote the first base of the 3'UTR after the end of the open reading frame. The "quality" of the seed site is given as n:w:m where n=number of base-pairs; w=wobbles; m=mismatches. All seed regions with 7 matches and over are listed, while 6-mer seed regions are listed only if they contain no mismatches and no wobbles. The free energy of miRNA:UTR binding is given and binding events are considered more likely when the ratio of ddG:dGopen is close to 1.